Research article

JGS
Journal of the Geological Society

https://doi.org/10.1144/jgs2025-034 | Vol. 183 | 2025 | jgs2025-034

From rift to continental collision: insights into the crustal evolution of the Southern Borborema Province (NE Brazil) revealed from metasedimentary rocks of the Sergipano Orogenic System

Fábio S. Pereira[1,2*], Jean-Michel Lafon[1], Maria L. S. Rosa[2], Herbet Conceição[2], João M. Milhomem Neto[1] and Moacyr M. Marinho[3]

[1] Programa de Pós-Graduação em Geologia e Geoquímica, Laboratório de Geologia Isotópica, Instituto de Geociências, Universidade Federal do Pará, 66075-110 Belém, Pará, Brazil
[2] Programa de Pós-Graduação em Geociências e Análise de Bacias, Universidade Federal de Sergipe, 49100-000 São Cristóvão, Sergipe, Brazil
[3] Instituto de Geociências, Universidade Federal da Bahia, 40170-290 Salvador, Bahia, Brazil
FSP, 0000-0002-8496-6501; J-ML, 0000-0003-0854-3053; MLSR, 0000-0002-5099-829X; HC, 0000-0002-9172-4519; JMMN, 0000-0003-0674-5102; MMM, 0000-0002-2143-5594
* Correspondence: fabiopereira@ufpa.br

Abstract: The Macururé Domain, the largest unit of the Sergipano Orogenic System in NE Brazil, comprises a supracrustal succession intruded by numerous Brasiliano/Pan-African plutons. In this study, we present U–Pb and Lu–Hf isotopic data on detrital zircon from quartzites, integrated with lithological, geochemical and published geochronological results, to constrain provenance and tectonic setting. Detrital zircon U–Pb spectra show prominent peaks at 2000–1980 and 1000–950 Ma, which correspond to the Paleoproterozoic Orogeny and the Cariris Velhos event. The Paleoproterozoic grains, with $\varepsilon_{Hf}(t)$ values ranging from −15.6 to +0.5, and Archean model ages of 3.5–2.5 Ga indicate that crustal reworking dominated during Paleoproterozoic source formation. Tonian grains, with $\varepsilon_{Hf}(t)$ values from −24.7 to +8.4 and model ages of 3.2–1.3 Ga, suggest contributions from both juvenile crust and ancient reworked components. These isotopic signatures differ from those of the São Francisco Craton and instead point to sources within the Borborema Province. The youngest grains (808–739 Ma) are contemporaneous with sedimentation and magmatism in the adjacent Canindé Domain, supporting a coeval basin development in an extensional setting, followed by basin inversion and continental collision at the onset of the Ediacaran.

Supplementary material: Supplementary material with analytical methods, figures, and data tables is available at https://doi.org/10.6084/m9.figshare.c.8092568

Thematic collection: This article is part of the New perspectives on South American Geology: a tribute to Emeritus Professor Reinhardt A. Fuck collection available at: https://www.lyellcollection.org/topic/collections/new-perspectives-on-south-american-geology

Received 26 January 2025; **revised** 23 September 2025; **accepted** 10 October 2025

This work is dedicated to Professor Reinhard A. Fuck, whose visionary contributions to the tectonic evolution of South America have shaped generations of geological research.

Zircon is a common minor component of clastic rocks that survives the sedimentary cycle due to its physicochemical stability and refractory character, ultimately becoming the last record of eroded ancient areas (e.g. Wilde *et al.* 2001). The high concentration of U–Th–Pb makes this heavy mineral a powerful tool for geochronological studies applied to sedimentary provenance and crustal evolution (Hoskin and Schaltegger 2003; Gehrels 2011; Cawood *et al.* 2012).

The standard application of this technique aims to provide time constraints on the sedimentation period, in which the youngest clastic constituent yields an estimate of the maximum depositional age (Coutts *et al.* 2019; Vermeesch 2021). This approach is important for Precambrian strata, where biostratigraphic age control is absent (Gehrels 2011). Potential source areas can be identified by matching detrital ages with known igneous and metamorphic zircon-forming events (Andersen *et al.* 2018). In addition, the age distribution patterns observed in detrital zircon spectra are directly linked to the tectonic setting of the basin in which the sediments were deposited (Cawood *et al.* 2012), enabling the elucidation of broad aspects of the geodynamic evolution of a region.

Besides the distribution of ages, the proportion of juvenile and recycled material plays a key role in understanding the genesis of a crustal segment. Once zircon preserves the Hf isotope signature of the magma source from which it crystallized, combining detrital ages and Lu–Hf isotope compositions is a valuable tool for distinguishing protosources with the same crystallization age (Griffin *et al.* 2004). When integrated with whole-rock geochemistry and lithological data, these isotopic tools allow a more robust characterization of source areas, capturing not only their timing of formation but also their compositional and tectonic nature (Nesbitt and Young 1984; Floyd and Leveridge 1987). This combined approach plays a key role in ancient orogenic systems, where complex interactions between cratonic blocks, arc systems and rift-related magmatism demand multiple, complementary lines of evidence to trace provenance.

The Sergipano Orogenic System (SOS), located in the southernmost segment of the Borborema Province, is part of a large Brasiliano/Pan-African orogen that extends to the Central African Orogenic Belt (Van Schmus *et al.* 2008; Caxito *et al.* 2020*b*). Most geodynamic reconstructions of this area have been based on geochemical and isotopic signatures of magmatic rocks (Oliveira *et al.* 2010; Pereira *et al.* 2023). In a pioneering work, Oliveira *et al.* (2015*b*) defined a general provenance framework for the main metasedimentary successions comprising the SOS. Subsequent studies (Lima *et al.* 2018; Neves *et al.* 2019; Passos *et al.* 2022) expanded the regional database with U–Pb zircon ages of igneous and sedimentary rocks, and a large number of *in situ* analyses are now available.

The Macururé Domain is the most prominent geological unit of the SOS. It consists mainly of the Macururé Complex, which includes a metasedimentary succession of phyllites and schists interlayered with thick successions of quartzite, intruded by late Cryogenian–Ediacaran plutonic rocks (Davison and Santos 1989; Silva *et al.* 1995). In this work, we adopt an integrated approach, combining the first coupled U–Pb and Lu–Hf analyses on detrital zircon with lithological and geochemical data from metasedimentary rocks of the Macururé Complex. These newly acquired data are integrated with the existing detrital zircon database of the SOS. This study aims to: (i) determine the provenance and tectonic setting of its metasedimentary rocks through detrital zircon geochronology and Hf isotopes; (ii) assess source-to-sink connections between the Macururé Domain and neighbouring domains of the SOS using integrated geochronological, isotopic and geochemical evidence; and (iii) propose a tectonic model for sedimentation within the regional context of the Southern Borborema Province.

Geological setting

Borborema Province

The Borborema Province in NE Brazil formed through the convergence of the Amazonian, São Luís–West Africa and São Francisco–Congo cratons during the assembly of Western Gondwana in the course of the Brasiliano/Pan-African Orogeny (Fig. 1a) (Brito Neves *et al.* 2000; Caxito *et al.* 2020*a*).

The basement of the Borborema Province is mainly composed of Paleoproterozoic orthogneisses related to the Rhyacian Orogeny (2.2–2.0 Ga) and localized Archean nuclei (Van Schmus *et al.* 2011; Rosa *et al.* 2020). Late Paleoproterozoic associations in the central and northern subprovinces are interpreted as extension-related magmatism emplaced during the Statherian–Calymmian transition (Amaral *et al.* 2015; Lages *et al.* 2019). Metavolcanic–sedimentary sequences and orthogneisses, correlated with the Cariris Velhos event (1.0–0.9 Ga), have been recognized in the Central and Southern sectors of the Borborema Province (Brito Neves *et al.* 1995; Carvalho 2005; Guimarães *et al.* 2016; Caxito *et al.* 2020*b*). In addition, late Neoproterozoic supracrustal successions covering the basement were intruded by widespread Brasiliano/Pan-African magmatism (650–530 Ma) represented by several batholiths, stocks and dyke swarms (Neves *et al.* 2015; Amorim *et al.* 2018).

The continental-scale Patos and Pernambuco shear zones are considered major crustal limits that divide the Borborema Province into Northern, Central and Southern subprovinces (Van Schmus *et al.* 2008, 2011). The Southern Subprovince is bounded to the north by the Pernambuco shear zone and to the south by the São Francisco Craton (SFC), and includes the Pernambuco-Alagoas Domain (PEAL), and the Sergipano and Riacho do Pontal orogenic belts (Fig. 1b).

Sergipano Orogenic System

The SOS has a triangular shape, and stands between the PEAL and SFC, corresponding to the western sector of the Central Africa Orogenic Belt (CAOB) in pre-drift reconstructions (Castaing *et al.* 1994; Caxito *et al.* 2020*a*). The SOS was formed by the amalgamation of different crustal segments with ages ranging from Rhyacian to late Ediacaran during the closure of a basin along the northern margin of the São Francisco Craton (Oliveira *et al.* 2010; Pereira *et al.* 2023).

From north to south, the SOS is divided into the Canindé, Poço Redondo, Marancó, Macururé, Vaza Barris and Estância domains (Davison and Santos 1989), separated by regional shear zones (Fig. 1c). The Estância, Vaza Barris and Macururé domains largely consist of metasedimentary rocks (Davison and Santos 1989; D'el-Rey Silva 1999), while the Marancó, Poço Redondo and Canindé domains include abundant magmatic and metasedimentary rock types, whose metamorphism conditions reach amphibolite facies (Oliveira *et al.* 2010). Figure 2 shows a simplified stratigraphy of the SOS, and Supplementary Table S1 summarizes the available detrital zircon geochronological data for its metasedimentary successions.

The Canindé Domain consists of: (i) Tonian basement slices (1006–989 Ma: Passos *et al.* 2022); (ii) the metavolcanic–sedimentary sequence of the Novo Gosto unit and a bimodal association of the Gentileza unit (743–701 Ma: Passos *et al.* 2021, 2022); (iii) a 719–704 Ma layered gabbroic complex (Pinto *et al.* 2020; Passos *et al.* 2022); and (iv) a suite of Brasiliano granitoids (640–611 Ma: Oliveira *et al.* 2015*a*; Santos 2016; Soares *et al.* 2019). Detrital zircon geochronological data for the Novo Gosto unit show a dominance of Tonian grains, with less expressive Rhyacian and Cryogenian contributions (Oliveira *et al.* 2015*b*; Passos *et al.* 2022). The youngest detrital zircon displays an age of 625 Ma, suggesting that sedimentation may have occurred synchronously with the Brasiliano/Pan-African Orogeny (Oliveira *et al.* 2015*b*).

The Marancó and Poço Redondo domains comprise Tonian migmatites (980–960 Ma) and A-type orthogneisses (967–940 Ma), intruded by Brasiliano granitoids between 636 and 617 Ma (Carvalho 2005; Oliveira *et al.* 2010, 2015*a*; Lima 2016; Lima *et al.* 2024). Quartzite and metaconglomerate samples from the Marancó Domain yielded a roughly unimodal distribution of detrital zircon data at 1000–980 Ma, indicating massive erosion of Tonian source areas (Oliveira *et al.* 2015*b*).

The Macururé Domain comprises the central and northern portions of the SOS, extending for *c.* 350 km across eastern Sergipe and northern Bahia. It consists of metasupracrustal rocks of the Macururé Complex, metamorphosed in greenschist–amphibolite facies, and an intrusive suite ranging from mafic–ultramafic to granitic rocks (643–603 Ma: Oliveira *et al.* 2015*a*; Pereira *et al.* 2023). The Macururé Complex includes phyllites, schists, metarhythmites and metagreywackes, interleaved with quartzite and calc-silicate rocks. U–Pb detrital zircon data for the Macururé Complex reveal a heterogeneous provenance dominated by Rhyacian and Tonian contributions (Van Schmus *et al.* 2011; Oliveira *et al.* 2015*b*; Neves *et al.* 2019). These authors argued for a pre-Brasiliano deposition for the sedimentary succession based on the absence of zircon grains younger than 900 Ma (Oliveira *et al.* 2015*b*).

The Vaza Barris and Estância domains encompass an anchimetamorphic to low-grade psammopelitic and carbonate sequence (Davison and Santos 1989). U–Pb detrital zircon data reveal distinct detrital age spectra from the base to the top of the successions, with a predominance of Rhyacian ages in the lowermost units, followed by increasing contributions of Tonian, Cryogenian and Ediacaran ages towards the top (Oliveira *et al.* 2015*b*).

Structural windows of Archean–Paleoproterozoic basement are exposed within the metavolcano-sedimentary successions of the Vaza Barris and Macururé domains (Fig. 1c). The Mesoarchean crystalline cores of the Simão Dias and Itabaiana domes consist of migmatitic orthogneisses with tonalite–trondhjemite–granodiorite affinities, yielding crystallization ages between 2.86 and 2.73 Ga (Oliveira 2012; Santiago *et al.* 2018; Rosa *et al.* 2020). The Jirau do Ponciano Dome comprises basic–acidic metavolcanic (2.07–

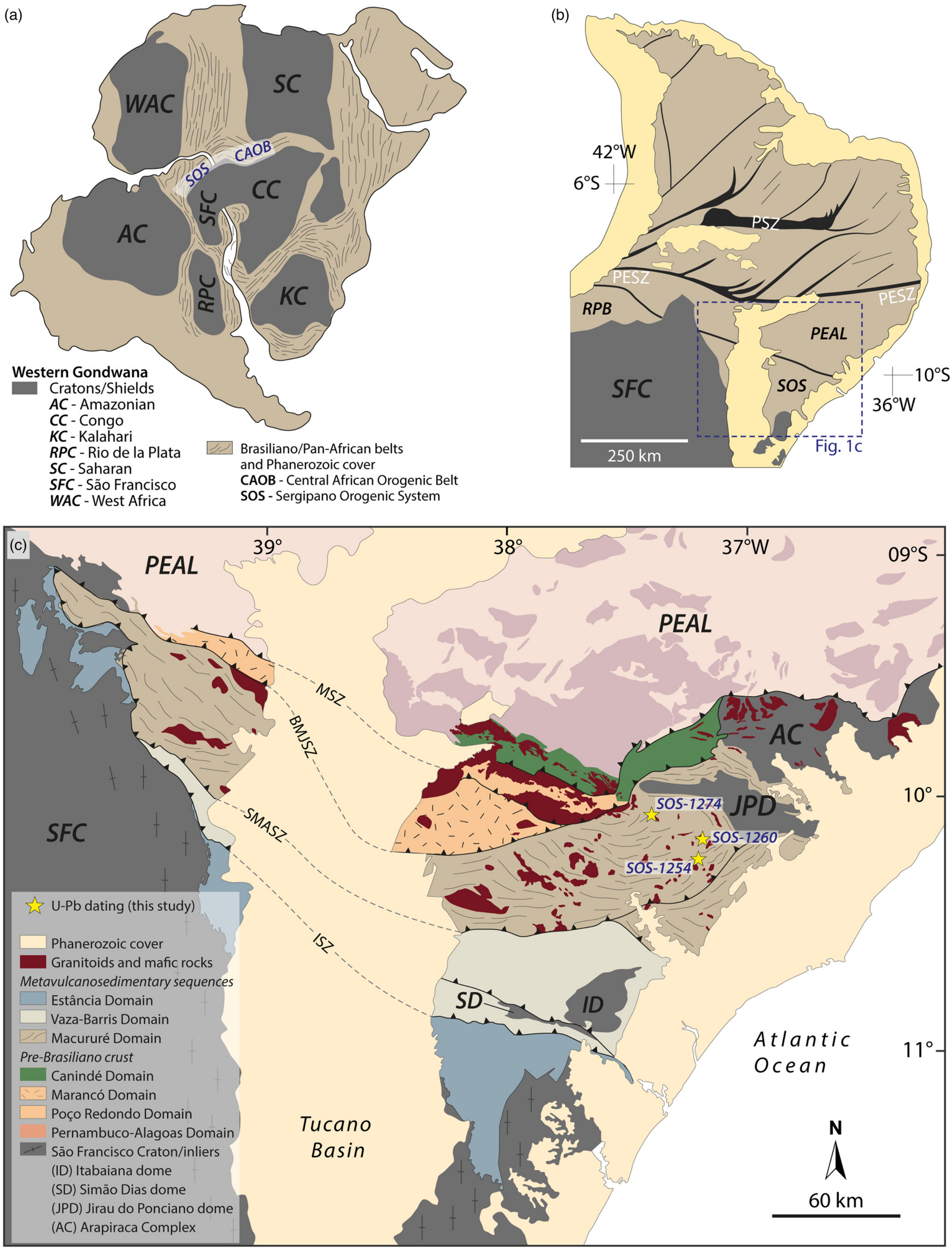

Fig. 1. Geological framework of the study area. (**a**) South America–Africa connection along the western margin of the Gondwana supercontinent, with the position of the main cratonic blocks. The outlined area corresponds to the extent of the Sergipano and Central African orogenic belts. (**b**) Division of the Borborema Province into the Northern, Central and Southern subprovinces, bounded by the Patos (PSZ) and Pernambuco (PESZ) shear zone systems. PEAL, Pernambuco-Alagoas Domain; RPB, Riacho do Pontal Belt. (**c**) Tectonic compartmentalization of the Sergipano Orogenic System (SOS). The Itaporanga Shear Zone (ISZ), São Miguel do Aleixo Shear Zone (SMASZ), Belo Monte-Jeremoabo Shear Zone (BMJSZ) and Macururé Shear Zone (MSZ) mark the limits between the domains. Source: (b) from Van Schmus *et al.* (2008, 2011); and (c) Davison and Santos (1989).

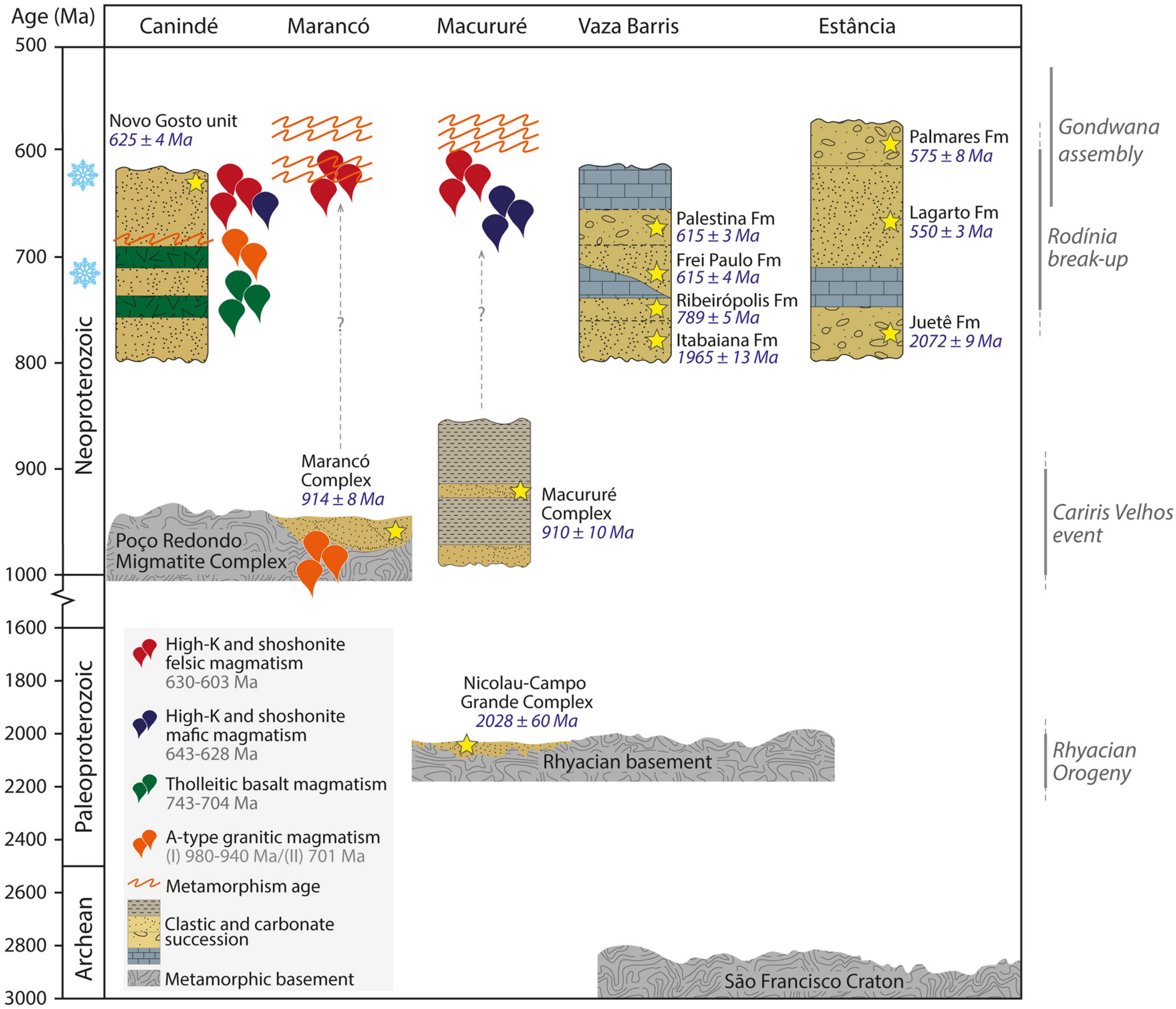

Fig. 2. Simplified stratigraphy and event chart based on available geochronological data for the Sergipano Orogenic System (SOS). Maximum depositional ages (yellow stars) refer to the youngest single grain of the formation or informal unit (see Supplementary Table S1). Middle Cryogenian (Sturtian) and late Cryogenian (Marinoan) glaciations are marked at *c.* 720 and *c.* 635 Ma. Source: São Francisco Craton (Oliveira 2012; Rosa *et al.* 2020), Rhyacian basement (Lima *et al.* 2019; Tesser *et al.* 2022), Tonian migmatites and granitoids (Carvalho 2005; Lima *et al.* 2024), pre-Brasiliano metamafic and metagranitoids (Pinto *et al.* 2020; Passos *et al.* 2021, 2022), Brasiliano mafic rocks and granitoids (Oliveira *et al.* 2015*a*; Pereira *et al.* 2020, 2023, 2024), metasedimentary sequences (Van Schmus *et al.* 2011; Oliveira *et al.* 2015*b*; Lima *et al.* 2018, 2019; Neves *et al.* 2019; Passos *et al.* 2022); the metamorphic ages are after Oliveira *et al.* (2010) and Passos *et al.* (2022); the middle (Sturtian) and late Cryogenian (Marinoan) glaciation ages are according to Hoffman *et al.* (2017).

2.05 Ga) and metasedimentary rocks of the Nicolau-Campo Grande Complex, interpreted as remnants of a Rhyacian–Orosirian continental arc (Lima *et al.* 2019). At the northern limit of the SOS, ultrahigh-temperature diatexites of the Arapiraca Complex (2.03–1.96 Ga) are considered a continental fragment pulled away from the São Francisco–Congo palaeocontinent (Tesser *et al.* 2022).

Analytical methods

The analytical techniques employed in this study were: (1) X-ray fluorescence (XRF) and inductively coupled plasma mass spectrometry (ICP-MS) for whole-rock major and trace element analyses; (2) laser ablation-quadrupole ICP-MS (LA-Q-ICP-MS) for U–Pb dating of detrital zircon; and (3) laser ablation-multicollector ICP-MS (LA-MC-ICP-MS) for Lu–Hf isotopic analyses of zircons. Detailed analytical procedures are provided in the Supplementary material.

Results

Geological outline of the Macururé Complex

In the eastern sector of the Macururé Domain, garnet-bearing muscovite–chlorite–biotite phyllites and metarhythmites are predominant, accompanied by subordinate garnet–mica schists, metagreywackes and metacarbonate rocks. Centimetre-to-metre layers of impure quartzite are interbedded with the phyllites and schists. Prominent hills near the cities of Nossa Senhora de Lourdes and Porto da Folha are defined by thick sequences of muscovite-rich quartzites, which exhibit complex fold interference patterns due to multiple deformation events (Bueno *et al.* 2009). Table 1 summarizes the main mineralogical and textural features of the analysed metasedimentary rocks.

Phyllites are grey, brown or reddish in colour, with a characteristic lustrous appearance. They contain idioblastic garnet porphyroblasts

Table 1. Petrographical characteristics of the metasedimentary rocks from the Macururé Complex

Rock group	Texture	Mineral assembly	
		Major	Accessory
Phyllite	Lepidoblastic, porphyroblastic, poikiloblastic	Qz + Pl + Ms + Bt + Chl + Grt	Tur ± Opq
Schist	Lepidoblastic, porphyroblastic, poikiloblastic	Ms + Bt + Qz + Pl + Grt ± Chl	Tur
Metarythmite	Lepidodoblastic, porphyroblastic	Ms + Chl + Bt + Qz + Kfs + Pl ± Grt	Zrn ± Opq
Metagreywacke	Porphyroclastic	Qz + Pl + Kfs + Ms + Chl ± Opq ± Cal	Rt + Zrn ± Tur
Metarcarbonate	Granoblastic, lepidoblastic	Cal + Ms + Chl + Qz + Kfs + Pl	Zrn ± Opq
Quartzite	Granoblastic, porphyroclastic, lepidoblastic	Qz + Pl + Kfs + Ms	Bt + Chl ± Ap ± Rt ± Zrn

Mineral abbreviations follow the recommendation of Warr (2021).

ranging from 0.2 to 0.5 mm in size. Foliation is defined by reddish-brown biotite crystals (*c.* 0.5 mm), which are partially altered to chlorite. The matrix comprises very-fine-grained (<0.01 mm) quartz, plagioclase and microcline. Muscovite and chlorite are aligned along the schistosity within the matrix. Accessory phases include disseminated opaque minerals and green tourmaline prisms.

Schist samples are medium grained and typically display a well-developed lepidoblastic texture defined by the alignment of biotite and muscovite (Fig. 3a). Garnet porphyroblasts are idioblastic, and contain inclusion trails of quartz, biotite and opaque minerals (Fig. 3b). Internal foliation within the garnet crystals is curved, suggesting syntectonic growth during prograde deformation. Fine-grained quartz and biotite also occur in pressure shadows around garnet. Quartz and plagioclase comprise granoblastic lenses orientated with the schistosity in some samples.

Metarhythmites exhibit a bimodal layering of millimetre-thick metapelite and metapsammite (Fig. 3c). The metapsammite consists of very-fine-grained quartz and feldspar, set in a matrix rich in muscovite, chlorite and some biotite. The metapelite layers primarily contain brown biotite, muscovite and sparse detrital grains. The alignment of mica blasts defines a slaty cleavage. Opaque minerals are the main accessories.

The metagreywackes (Fig. 3d) consist of poorly sorted quartz grains and minor amounts of feldspar, ranging from very fine to very coarse granulation, with a predominance of *c.* 0.3 mm. These grains are embedded in a recrystallized quartzofeldspathic matrix, including chlorite, muscovite and biotite. Rare tiny grains of green tourmaline, zircon and rutile are dispersed throughout. In addition, some samples include carbonate and opaque minerals associated with the matrix.

Fig. 3. Field and petrographical features of metasedimentary units from the Macururé Domain. (**a**) Medium-grained muscovite–biotite schist with conspicuous garnet porphyroblasts. (**b**) Lepidoblastic texture defined by the alignment of muscovite (Ms) and biotite (Bt) in (a), with quartz (Qz) pressure shadows around syntectonic garnet (Grt). (**c**) Alternating layers of fine-grained arenite (light grey) and siltite (dark grey) in metarhythmite. Tiny black spots in the siltite are oxidized garnet porphyroblasts. (**d**) Poorly sorted, fine- to medium-grained reddish metagreywacke, preserving faint sedimentary layering despite the metamorphic overprint. (**e**) Muscovite-rich quartzite displaying a well-developed foliation. (**f**) Thin section of (e), showing stretched quartz grains and aggregates with undulose extinction, and muscovite blasts defining a mylonitic, spaced foliation. Kfs, K-feldspar; Pl, plagioclase.

Metacarbonate rocks are light–medium grey marls featuring centimetre-thick intercalations of dark grey impure carbonates. Metamarls consist of fine-grained muscovite and chlorite (*c*. 0.2 mm), strongly orientated and situated between a polygonal calcite mosaic and quartz. Rare opaque minerals align with the mica orientation. Calcite veinlets are injected along the foliation. Impure metacarbonates display very-fine granulation (<0.1 mm) and comprise a polygonal mosaic of calcite, with interstices filled by muscovite, quartz and feldspar. Thin calc-silicate levels (1–10 cm) typically contain plagioclase, amphibole, epidote and quartz. Near intrusions, the calc-silicate rocks give place to a more massive structure and porphyroblastic texture, marked by the development of large crystals of amphibole and garnet.

Quartzites are light grey to yellowish and fine–medium grained (Fig. 3e). They are predominantly composed of xenoblastic, inequigranular quartz displaying a granoblastic texture. Muscovite is present in variable proportions, qualifying them as muscovite-bearing quartzites (<5 vol%) or muscovite quartzites (>5 vol%). These crystals define a poorly developed foliation, locally forming anastomosing networks around porphyroclasts of plagioclase and microcline, both of which are extensively altered to sericite. Minor biotite and opaque minerals occur in association with muscovite. Larger quartz grains commonly exhibit patchy undulose extinction and deformation lamellae, with interlobate to amoeboid grain boundaries. Fine-grained recrystallized quartz aggregates are present along these boundaries, indicating dynamic recrystallization. In some samples, well-developed foliation, elongated quartz grains and aligned muscovite define a mylonitic fabric (Fig. 3f).

In contrast to quartzofeldspathic rocks, pelitic protoliths undergo significant mineralogical transformations during metamorphism, making them more suitable for assessing metamorphic conditions. According to Bucher and Grapes (2011), garnet appears in metapelites at *c*. 450°C, and the first garnet–biotite pairs may form at *c*. 470°C. The observed mineral assemblage in phyllites and schists, therefore, indicates metamorphism under greenschist–lower amphibolite facies, corresponding to the garnet zone of Barrovian-type metamorphism. The absence of staurolite suggests that conditions did not exceed the lower amphibolite facies. The mylonitic fabric observed in quartzites is attributed to nappe tectonics, developed along low-angle shear zones with SW-directed mass transport, consistent with the main collisional structures of the SOS. Finally, the partial replacement of biotite by chlorite reflects retrograde metamorphic overprinting.

Geochemical characterization

Major and trace element results are given in Supplementary Table S2. Whole-rock geochemical data for phyllites, schists and greywackes show variable contents of SiO_2 (55.00–77.11 wt%), TiO_2 (0.57–1.16 wt%), Al_2O_3 (10.68–22.62 wt%), Fe_2O_3* (4.34–12.95 wt%), MgO (0.45–5.51 wt%), CaO (0.07–7.21 wt%), Na_2O (0.98–3.52 wt%), K_2O (1.47–4.95 wt%) and P_2O_5 (0.02–0.28 wt %). As the geochemical composition of these fine-grained, matrix-rich rocks overlaps widely, they are treated together here.

Quartzite samples differ from the others by their higher and narrower range of SiO_2 contents (88.64–92.33 wt%), moderate Al_2O_3 (4.76–7.00 wt%) and K_2O (1.90–2.82 wt%), and very low values of TiO_2 (<0.14 wt%), Fe_2O_3* (<1.17 wt%), MgO (<0.11 wt %), CaO (<0.01), Na_2O (<0.55 wt%) and P_2O_5 (<0.01%).

The contents of TiO_2, Al_2O_3, Fe_2O_3* and MgO decrease with increasing SiO_2, indicating the removal of unstable ferromagnesian components with the enhancement of sediment maturity (Fig. 4a–d). Conversely, K_2O, Na_2O and CaO display weak negative correlations with SiO_2 (Fig. 4e–g). Across all variation diagrams, the metapelites exhibit compositions similar to the Post-Archean Australian Shale (PAAS) (Taylor and McLennan 1985), whereas quartzite samples spread close to Proterozoic Cratonic Sandstone (Condie 1993). This behaviour indicates that quartzite protoliths were composed of more mature detritus relative to the protoliths of the metapelites and metagreywackes.

Phyllites, schists and metarhythmites show abundances of rare-earth elements (REEs) ranging from 89 to 305 ppm (128 ± 57 ppm on average), lower than the PAAS (184.8 ppm: Taylor and McLennan 1985). The analysed rocks are enriched by a factor of 100 and 10 times for the light REEs (LREEs) and heavy REEs (HREEs), respectively, relative to the chondrites (McDonough and Sun 1995). Chondrite-normalized (expressed by the subscript ‘CN’) REE patterns feature weak to moderate fractionation, with La/Yb_{CN} ratios between 3.6 and 13.4 (Fig. 4h). The fractionation degree is more pronounced among the LREEs (La/Sm_{CN} = 2.5–4.1) than the HREEs (Gd/Yb_{CN} = 0.9–2.3). They display virtually absent Ce anomalies (Ce/Ce* = 0.86–1.10) and significant negative Eu anomalies (Eu/Eu* = 0.42–0.77), which are typical features of post-Archean sedimentary rocks (Taylor and McLennan 1985).

The average concentration of ferromagnesian trace elements Ni (47 ± 16 ppm), Co (19 ± 11 ppm) and V (122 ± 32 ppm) are within the range reported for both PAAS and upper continental crust (UCC) (Taylor and McLennan 1985; Rudnick and Gao 2003). Trace element compositions of metapelitic rocks from the Macururé Complex normalized to the UCC are presented in Figure 4i. Most samples cluster near unity, with marked depletions in Sr and P. Overall, the concentrations of high-field strength elements (HFSEs) and large ion lithophile elements (LILEs) are similar to those of PAAS.

Detrital zircon U–Pb geochronology and Lu–Hf isotope geochemistry

Three quartzite samples from the Macururé Complex were analysed for U–Pb geochronology. Of the 370 detrital zircon grains initially dated, 247 yielded concordant ages with discordance of less than 10%. Lu–Hf isotopic compositions were obtained from 113 of these concordant grains. The complete U–Pb and Lu–Hf results are provided in Supplementary Tables S3 and S4, and a summary of the results is shown in Table 2.

Muscovite quartzite: sample SOS-1254

Sample SOS-1254 is a muscovite quartzite, cropping out as a 50 cm-thick layer intercalated with garnet-bearing biotite–muscovite phyllites near the external ring of the Nossa Senhora de Lourdes interference structure (Fig. 1c).

Zircon grains are colourless, pale pink and light grey, translucent, and rarely limpid. Their sizes range from 80 to 310 µm. Most grains are rounded to subrounded, with length/width ratios of 1:1 and 3:1. Only a few preserve their original prismatic shape (Fig. 5).

Of the 120 analysed grains, 80 yielded concordant results within 10%. They are anhedral to subhedral and show regular broad or fine oscillatory zoning (53%), typical of igneous zircon (Corfu 2003). The remaining grains are homogeneous (10%) under cathodoluminescence (CL) images or reveal complex internal structures, dominated by irregular diffuse (14%) and concentric (8%) zoning. Internal features showing chaotic (5%), convolute (5%) and patchy (4%) patterns are less common. No clear relationship was observed between zoning type and Th/U ratios, which vary from 0.24 to 2.04 (Fig. 6a).

Detrital zircon U–Pb dates range from Siderian to Tonian (Fig. 6b). The kernel density estimate (KDE) plot for the concordant and subconcordant populations shows an almost bimodal distribution, with prominent peaks at 2100–1900 and 1200–800 Ma (Fig. 6c). One subconcordant grain provided a Siderian $^{207}Pb/^{206}Pb$ date of 2354 ± 31 Ma.

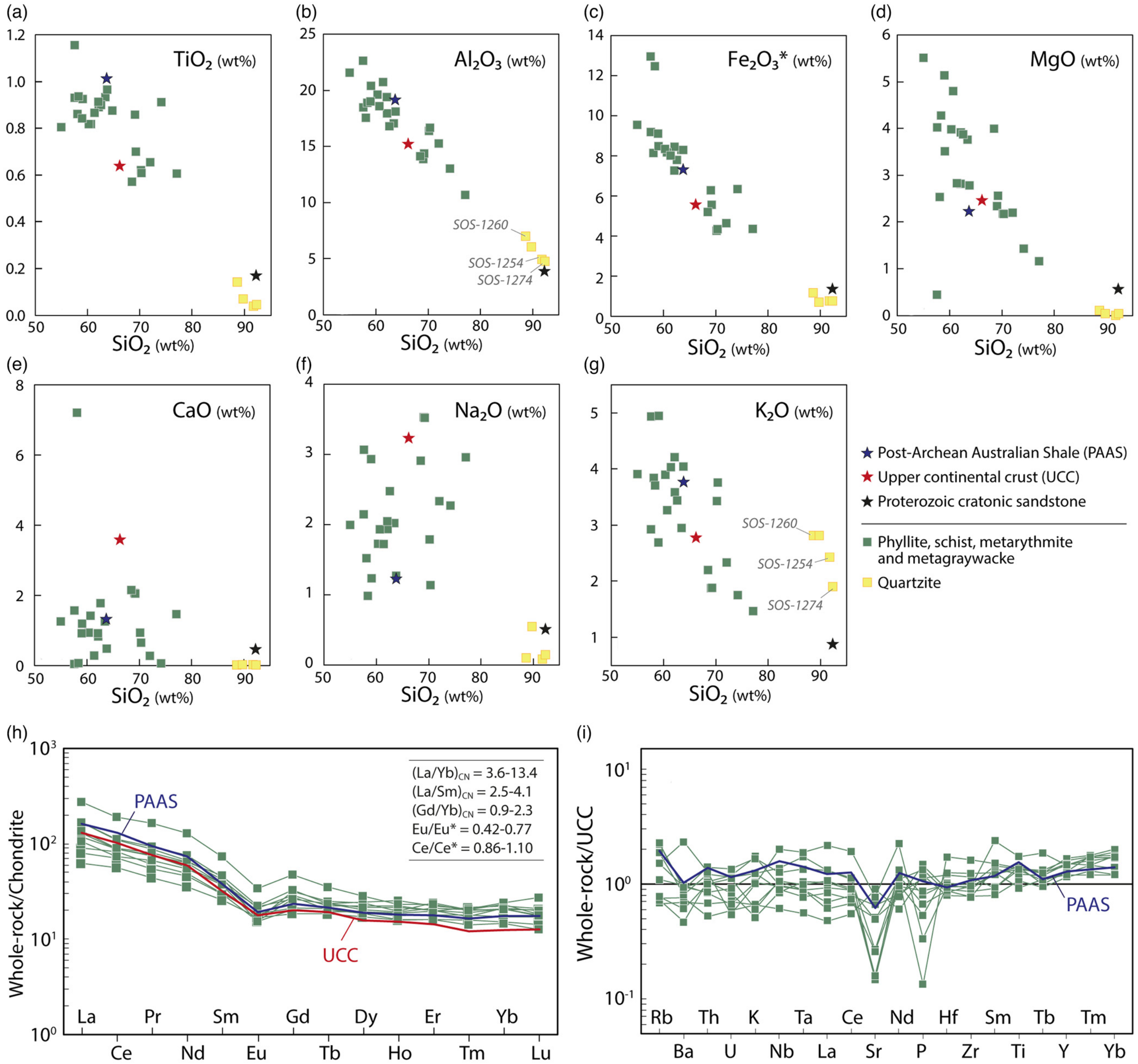

Fig. 4. Major and trace element geochemistry of metasedimentary rocks from the Macururé Complex. (**a**)–(**g**) Variation diagrams of selected oxides (wt%) plotted against SiO_2. The compositions of PAAS, UCC and Proterozoic cratonic sandstones are shown for comparison. (**h**) Chondrite-normalized REE patterns and (**i**) UCC-normalized multi-element diagrams for phyllites, schists and metarhythmite samples. Source: (a)–(g) compositions are from Taylor and McLennan (1985), Condie (1993) and Rudnick and Gao (2003); normalization values are after McDonough and Sun (1995) and Rudnick and Gao (2003).

About 40% of the grains are in the Rhyacian–Orosirian age interval, with a peak at 1980 Ma. They have subchondritic $^{176}Hf/^{177}Hf_{(t)}$ ratios between 0.281075 and 0.281517, equivalent to $\varepsilon_{Hf}(t)$ values from −15.6 to −0.7 (Fig. 6j). Hf-T_{DM}^{C} model ages spread from the Paleoarchean to the Neoarchean, ranging from 3.5 to 2.6 Ga (Fig. 6k).

The second cluster peaks at 960 Ma and contains zircon grains from the Mesoproterozoic (20%), early Neoproterozoic (28%) and middle Neoproterozoic (11%) intervals. $^{176}Hf/^{177}Hf_{(t)}$ ratios of the Mesoproterozoic grains vary from 0.281949 to 0.282289, recording negative to positive $\varepsilon_{Hf}(t)$ values between −7.1 and +5.1. They yielded Paleoproterozoic Hf-T_{DM}^{C} model ages ranging from 2.2 to 1.6 Ga.

The early Neoproterozoic population has varying $^{176}Hf/^{177}Hf_{(t)}$ ratios between 0.281851 and 0.282252, corresponding to subchondritic and suprachondritic $\varepsilon_{Hf}(t)$ values from −12.3 to +3.5. Hf-T_{DM}^{C} model ages range from 2.5 to 1.6 Ga.

The youngest zircon population records non-radiogenic $^{176}Hf/^{177}Hf_{(t)}$ ratios in the range of 0.281558 and 0.282069, equivalent to $\varepsilon_{Hf}(t)$ values from −24.7 to −6.0. Hf-T_{DM}^{C} model ages spread from the Mesoarchean to the Rhyacian (3.2–2.1 Ga). The youngest single grain yielded a $^{206}Pb/^{238}U$ date of 808 ± 13 Ma.

Mylonitic muscovite quartzite: sample SOS-1260

This sample is a mylonitic muscovite quartzite exposed in an operating quarry located in the external ring of the Nossa Senhora de Lourdes interference structure, along the road to the Escurial village (Fig. 1c).

Zircon grains are pale pink and light grey, mostly clear and less commonly translucent or opaque. Grain sizes range from 133 to 380 μm. Larger grains exhibit subrounded shapes but still preserve their original prismatic habit, whereas smaller grains are rounded and subspherical. Length/width ratios range from 3:1 to 1:1 (Fig. 5).

Table 2. Summary of U–Pb and Lu–Hf isotopic data from detrital zircon in quartzite samples of the Macururé Complex

Sample ID	Coordinates*	Concordant/analysed grains		900–701 Ma	1000–901 Ma	1600–1001 Ma	1800–1601 Ma	2300–1801 Ma	2500–2301 Ma	>2500 Ma
SOS-1254	718420/8879989	80/120	%	**11.3**	**27.5**	**20.0**	-	**40.0**	**1.2**	-
			$\varepsilon_{Hf}(t)$	−24.7 to −6.0	−12.3 to +3.5	−7.1 to +5.1		−15.6 to −0.7		
			Hf-T_{DM}^{C} (Ga)	3.2–2.1	2.5–1.6	2.2–1.5		3.5–2.6		
SOS-1260	720250/8889560	114/180	%	**16.7**	**40.3**	**14.9**	-	**27.2**	-	**0.9**
			$\varepsilon_{Hf}(t)$	−5.2 to +3.3	−10.3 to +4.4	−8.9 to +8.4		−10.4 to 0		
			Hf-T_{DM}^{C} (Ga)	1.9–1.5	2.4–1.5	2.4–1.3		3.1–2.5		
SOS-1274	693659/8901596	53/70	%	**7.5**	**26.4**	**17.0**	-	**49.1**	-	-
			$\varepsilon_{Hf}(t)$	−2.3	−1.0 to +7.7	−10.0 to +2.7		−9.0 to +0.5		
			Hf-T_{DM}^{C} (Ga)	1.8	1.8–1.3	2.4–1.7		3.1–2.5		

-, age interval not sampled.*Universal Transverse Mercator coordinate system, South American 1969 datum, 24S zone.

U–Pb zircon analyses performed on 180 detrital zircon grains returned 114 concordant to subconcordant dates within 10% of discordance. Most zircon grains display regular magmatic textures, such as oscillatory (63%) and sector (3%) zoning (Fig. 6d). Homogeneous unzoned grains account for 15% of the analysed population, while more complex zoning patterns make up 19% of the total (irregular concentric 8%, diffuse 5%, convolute 4%, and chaotic, cross-bedding and patchy *c.* 2%). Despite the diversity of internal structures, Th/U ratios do not vary significantly between the zoning types, ranging from 0.14 to 1.63.

Concordant and subconcordant U–Pb dates spread from the Mesoarchean to the Cryogenian, with two significant clusters at 2100–1900 and 1150–700 Ma (Fig. 6e, f). Only one xenocrystic core yielded an Archean $^{207}Pb/^{206}Pb$ date of 2904 ± 29 Ma. The older cluster encloses 27% of the grains and gives a peak on the KDE plot at 2000 Ma (Fig. 6f). Many of these grains show disturbed internal textures, consistent with late- to post-magmatic modification. Middle Paleoproterozoic grains yielded $^{176}Hf/^{177}Hf_{(t)}$ between 0.281302 and 0.281541, corresponding to subchondritic to chondritic $\varepsilon_{Hf}(t)$ values from −10.4 to +0.1 (Fig. 6j). Hf-T_{DM}^{C} model ages range from the Mesoarchean to the Neoarchean, between 3.1 and 2.5 Ga (Fig. 6k).

The younger cluster peaks at 950 Ma and represents 72% of the analysed population: 15% Mesoproterozoic, 40% Tonian and 17% middle Neoproterozoic. Most exhibit undisturbed internal structures compatible with a magmatic origin.

The Mesoproterozoic population displayed $^{176}Hf/^{177}Hf_{(t)}$ ratios ranging from 0.281836 to 0.282366, consistent with negative to positive $\varepsilon_{Hf}(t)$ values between −8.9 and +8.4, with Siderian–Ectasian Hf-T_{DM}^{C} model ages (2.4–1.3 Ga).

Representative grains of the Tonian period provided $^{176}Hf/^{177}Hf_{(t)}$ ratios between 0.281883 and 0.282285, equivalent to subchondritic and suprachondritic $\varepsilon_{Hf}(t)$ values ranging from −10.3 to +4.4. Hf-T_{DM}^{C} model ages vary from 2.4 to 1.3 Ga.

The middle Neoproterozoic group encloses grains with initial $^{176}Hf/^{177}Hf$ ratios between 0.282150 and 0.282333, corresponding to $\varepsilon_{Hf}(t)$ values from −5.2 to +3.3. Hf-T_{DM}^{C} model ages spread from the Orosirian to the Calymmian (1.8–1.5 Ga). The youngest single grain provided a $^{206}Pb/^{238}U$ date of 739 ± 14 Ma.

Muscovite-bearing quartzite: sample SOS-1274

Sample SOS-1274 is a muscovite-bearing quartzite exposed along the road near the Iguaçu locality. It belongs to a thick quartzite package that forms prominent hills between Gararu and Porto da Folha (Fig. 1c).

Detrital zircon grains are mostly clear and pale pink. Translucent and opaque brown grains are less common. Grains range from prismatic to spherical, but subrounded shapes predominate (Fig. 5). Length/width ratios vary between 4:1 and 1:1, and some grains contain inclusions of opaque minerals.

Seventy detrital zircon grains were dated, of which 53 are concordant within 10%. They are anhedral to subhedral. Oscillatory zoning (36%) and homogeneous unzoned (34%) structures prevail under CL. Less frequent patterns include irregular concentric (13%), diffuse (9%), chaotic (4%), convolute (2%) and sector (2%) zoning (Fig. 6g). Internal features related to secondary overprint are more common in the older population. Regardless of zoning type, Th/U ratios range from 0.07 to 1.54.

This sample displays a bimodal age distribution (Fig. 6h, i). Nearly half of the zircons (49%) yield Orosirian dates, defining two peaks at 2000 and 1800 Ma. This population has $^{176}Hf/^{177}Hf_{(t)}$ ratios ranging from 0.281283 to 0.281533, corresponding to $\varepsilon_{Hf}(t)$ values between −9.0 and +0.5 (Fig. 6j). Mesoarchean–Neoarchean Hf-T_{DM}^{C} model ages oscillate from 3.1 to 2.5 Ga (Fig. 6k).

Mesoproterozoic grains comprise 17% of the analysed concordant population. These grains show $^{176}Hf/^{177}Hf_{(t)}$ ratios between

Fig. 5. Cathodoluminescence (CL) images for representative detrital zircon grains from quartzite samples of the Macururé Domain. The scale bar corresponds to 50 µm. The grey and orange circles indicate the approximate location of the U–Pb and Lu–Hf spots, together with the U–Pb age (Ma), concordance (%) and Hf isotopic compositions ($\varepsilon_{Hf}(t)/T^{C}_{DM}$).

0.282071 and 0.282196, consistent with negative to positive $\varepsilon_{Hf}(t)$ values from −10.0 to +2.7. Hf-T^{C}_{DM} model ages spread from the Siderian to the Statherian (2.4–1.7 Ga).

The remaining 34% of detrital grains are clustered in the early (26%) and middle (8%) Neoproterozoic interval ages, marking a prominent peak at 1000 Ma and a subordinate 750 Ma. Early Tonian zircons record $^{176}Hf/^{177}Hf_{(t)}$ values from 0.282137 to 0.282385, equivalent to subchondritic to suprachondritic $\varepsilon_{Hf}(t)$ values between −1.0 and +7.7. Their Hf-T^{C}_{DM} model ages range from 1.8 to 1.3 Ga.

One middle Neoproterozoic grain analysed for Lu–Hf gave a negative $\varepsilon_{Hf}(t)$ value of −2.3 ($^{176}Hf/^{177}Hf_{(t)} = 0.282192$) and an Orosirian Hf-$T^{C}_{DM}$ model age of 1.8 Ga. The youngest single grain yielded a $^{206}Pb/^{238}U$ date of 782 ± 12 Ma.

Discussion

On the protolith compositions, weathering conditions and source characteristics

The bulk-rock geochemistry of siliciclastic rocks is controlled by a complex interplay of protolith composition, source characteristics and tectonic setting, modulated by weathering, transport and

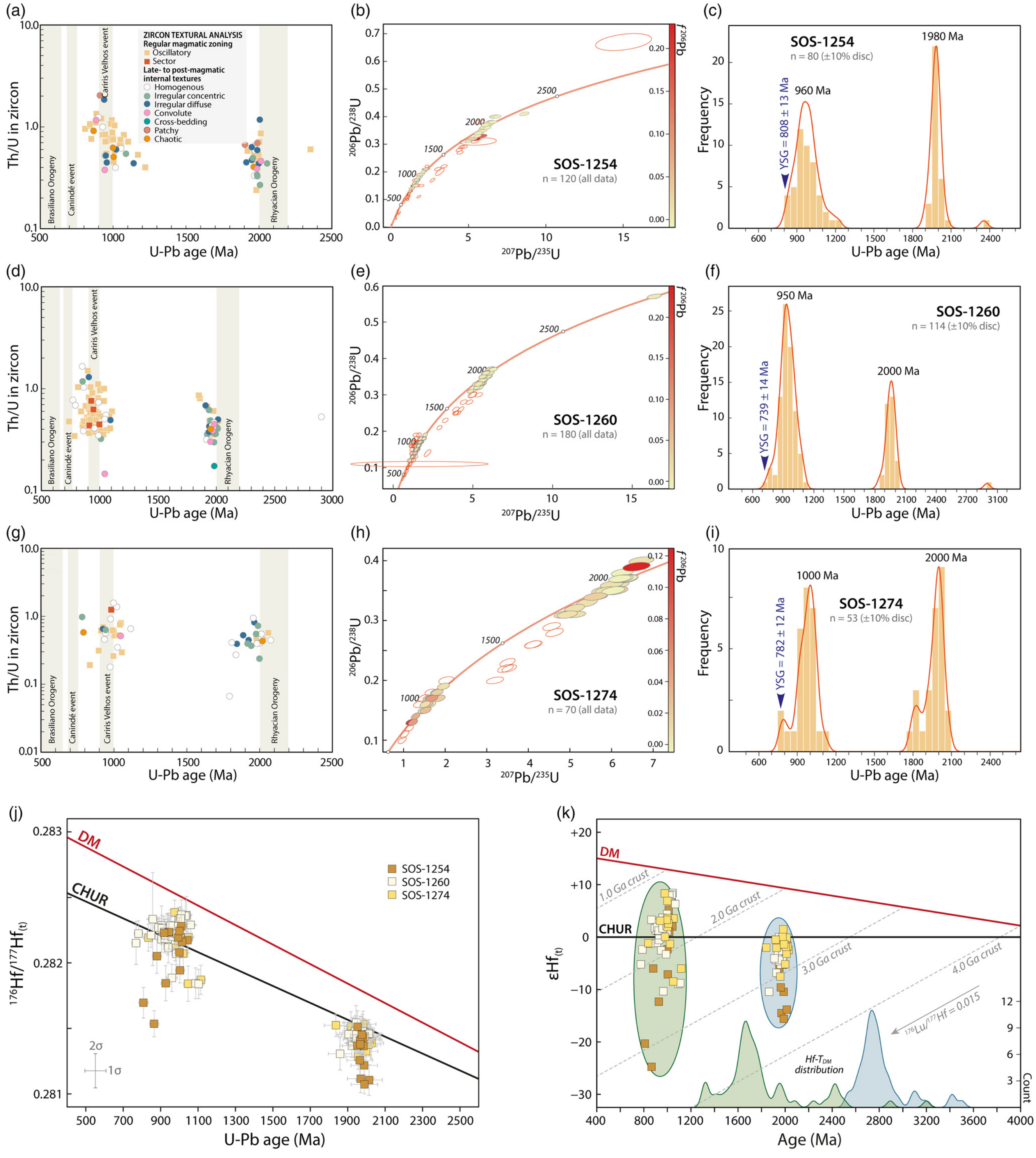

Fig. 6. Detrital U–Pb data for quartzite samples from the Macururé Domain. (**a**), (**d**) and (**g**) Textural features of concordant and subconcordant zircon grains relative to their U–Pb dates and Th/U ratios. (**b**), (**e**) and (**h**) Wetherill concordia diagrams displaying all analysed data. Discordant data are shown as hollow ellipses. Concordant data within 10% are shaded according to the proportion of common Pb for each analysed spot, expressed as absolute values of f_{206}. (**c**), (**f**) and (**i**) KDE plot with the main age peaks and the youngest single grain (YSG). Plots of U–Pb age v. (**j**) $^{176}Hf/^{177}Hf_{(t)}$ and (**k**) $\varepsilon_{Hf}(t)$. Crustal evolution trends in (k) assume a $^{176}Lu/^{177}Hf$ ratio of 0.015 for average continental crust. KDE plots also show the distribution of Hf-T^{C}_{DM} model ages for the two main zircon populations. CHUR, chondritic uniform reservoir; DM, depleted mantle. Source: (k) ratio from Griffin *et al.* (2004).

diagenesis (Nesbitt and Young 1982; Taylor and McLennan 1985; McLennan *et al*. 1993; Fedo *et al*. 1995; Rollinson and Pease 2021). This implies that geochemical data on clastic sediments is a helpful tool for characterizing processes such as hydraulic sorting, chemical weathering and detrital mineralogy of the source region (Rollinson and Pease 2021).

The degree of maturity of the studied samples can be visualized in a ternary plot of ferromagnesian oxides, silica and alkalis, which shows an increase from metapelites and metagreywackes to quartzites (Fig. 7a). Prolonged weathering breaks down the unstable mafic minerals, depleting sediments of ferromagnesian components, while the destabilization of feldspars and micas impoverishes the alkali content (Rollinson and Pease 2021). This increases the volume of residual quartz, leading to the high levels of compositional maturity observed in quartzites. In the classification scheme for siliciclastic rocks by Herron (1988), metapelites and metagreywackes plot in the

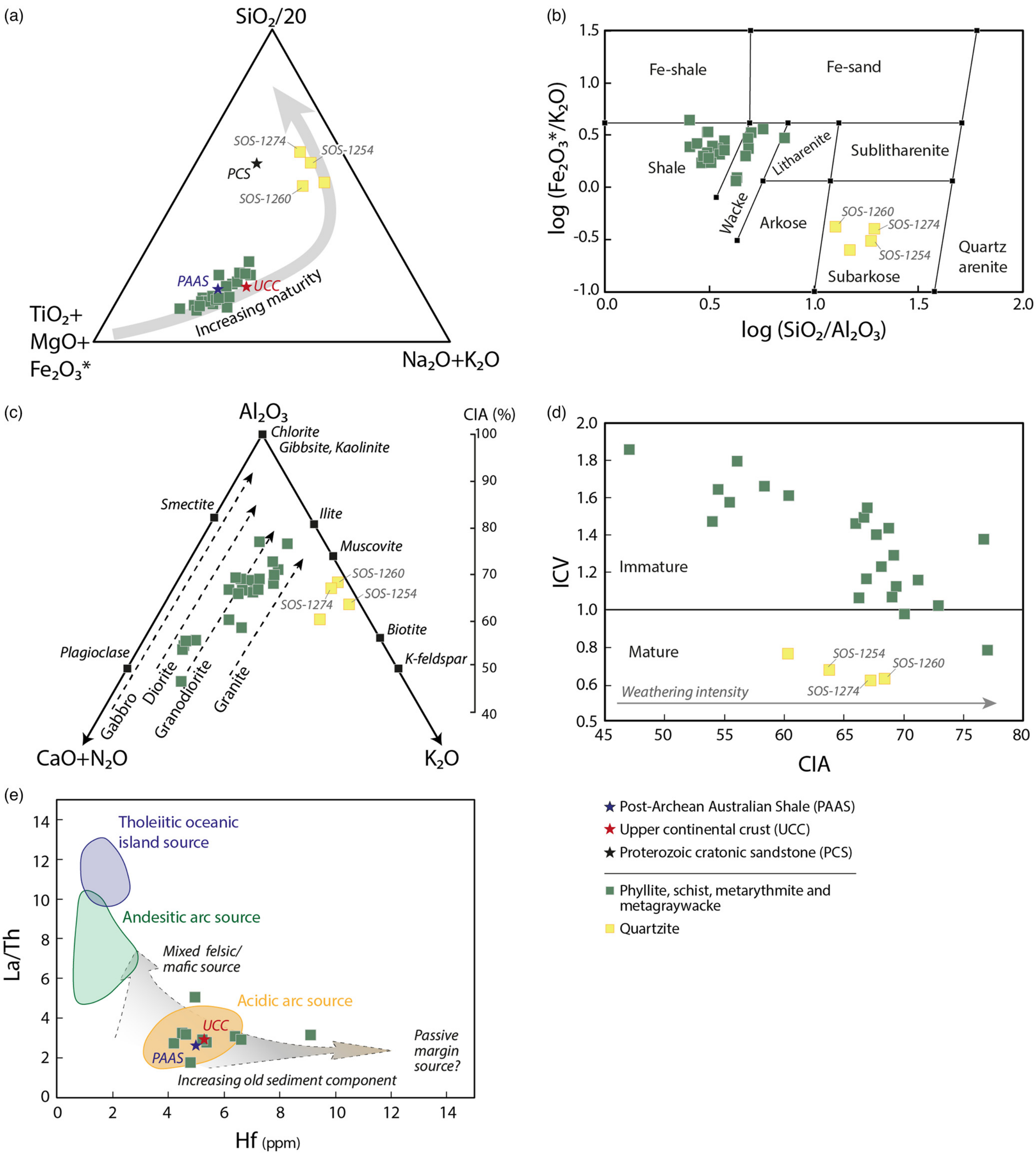

Fig. 7. Geochemical constraints on the protolith, weathering and source characteristics. (**a**) $TiO_2 + MgO + Fe_2O_3$*–SiO_2/20–$Na_2O + K_2O$ ternary diagram showing the trend of increasing maturity. (**b**) Plot of log(SiO_2/Al_2O_3) v. log(Fe_2O_3/K_2O) for the classification of the sedimentary protoliths. (**c**) Compositional space $CaO + Na_2O$–Al_2O_3–K_2O with poles of the main minerals and typical rock types. The dashed grey arrows indicate the weathering trends of various igneous rocks. (**d**) Plot of chemical index of alteration (CIA) v. index of compositional variability (ICV) parameters to infer the intensity of weathering and the degree of maturity of source areas. (**e**) Source and compositional discrimination in terms of the La/Th ratio and Hf abundance. Source: (a) from Kroonenberg (1990); (b) from Herron (1988); (c) from Nesbitt and Young (1984); (d) from Nesbitt and Young (1982) and Cox *et al.* (1995); and (e) from Floyd and Leveridge (1987).

shale and wacke fields, consistent with immature sedimentary protoliths. Otherwise, the quartzites fall within the subarkose field (Fig. 7b).

The chemical index of alteration (CIA) is a good measure of chemical weathering (Nesbitt and Young 1982), defined as CIA = 100 × molar [$Al_2O_3/(Al_2O_3 + CaO^* + Na_2O + K_2O)$], where CaO* corresponds to CaO in the silicate fraction of the sample. CIA values for the metapelitic rocks vary from 47 to 77 (65 ± 7 on average) and overlap the range observed in the quartzites (60–68; 67 ± 6 on average), indicating minimal to moderate chemical weathering. In the ($CaO^* + Na_2O$)–Al_2O_3–K_2O compositional space, the metapelites plot mainly along the weathering line of granodiorite composition (Nesbitt and Young 1984), suggesting derivation from intermediate to acidic source areas (Fig. 7c). The quartzite samples lie away from metapelites and approximate the Al_2O_3–K_2O joint, which may reflect the feldspar content in the protoliths (Bahlburg and Dobrzinski 2011).

The index of compositional variability (ICV), where ICV = (Fe_2O_3 + K_2O + Na_2O + CaO + MgO + MnO + TiO_2)/Al_2O_3, is an effective measure of the compositional maturity of source rocks (Cox *et al.* 1995). Quartzites yield ICV values <1.0 (0.62–0.77; 0.68 ± 0.06 on average), consistent with compositionally mature subarkose protoliths (Fig. 7d). Except for two samples, the ICV values for the metapelitic rocks are consistently above 1.0 (0.98–1.86; 1.36 ± 0.27 on average), indicating that metapelitic protoliths were dominated by immature sediments. Thus, we argue that the detritus constituting the quartzites does not record a simple source-to-sink history but rather successive episodes of erosion and sedimentation. However, the metapelites and metagreywackes certainly represent compositionally immature, first-cycle deposits.

Igneous rocks formed in active continental margins typically show high contents of incompatible elements (e.g. LILEs and LREEs), strongly negative Eu and Nb–Ta anomalies, and low contents of transition metals (e.g. Ni, V and Co) related to extensive magma fractionation (Pearce 1982; Wilson 1989). In such settings, immature clastic rocks retain the composition of proximal sources due to the presence of unstable grains and lithic fragments (Floyd and Leveridge 1987; Rollinson and Pease 2021). Phyllite, schist and metarhythmite samples show high and variable LILE concentrations, and REE patterns moderately enriched in LREE, with pronounced negative Eu anomalies and nearly flat HREEs. These features are typical of felsic–intermediate rocks from mature continental arcs, rather than young and undifferentiated arcs (McLennan *et al.* 1993). Figure 7e indicates that immature samples have low La/Th ratios at moderate Hf concentrations, akin to those observed in acidic-dominated arcs (Floyd and Leveridge 1987). Thus, the geochemical evidence suggests that the source materials for the metapelite samples were primarily composed of felsic igneous rocks exhibiting an arc-like signature.

Detrital zircon record

A detailed examination of the internal features of the dated grains demonstrates the dominance of regular concentric zoning, characteristic of igneous zircon crystals (Corfu 2003). Homogenous unzoned patterns represent the second most common feature, followed by disturbed zonation structures, such as convolute, chaotic and diffuse zoning (Fig. 6). These complex patterns are more frequent in the older zircon population, suggesting late- to-post-magmatic transformations related to metamorphic overprint or interaction with aqueous fluids (Corfu 2003; Rubatto 2017). In contrast, most zircon grains with well-preserved oscillatory zoning occur in the younger age fraction. These grains tend to be less rounded, with some retaining prismatic and pyramidal faces, indicating either short transport distances or limited residence time in surface environments.

Depositional ages

Given that a sedimentary deposit cannot be older than its youngest constituents, the age of this component can be used to constrain its maximum depositional age (MDA) (Gehrels 2011, 2014; Coutts *et al.* 2019). However, commonly used methods for deriving the MDA from detrital zircon populations (e.g. youngest single grain, youngest graphical peak or youngest grain cluster) often underestimate or overestimate depositional estimates (Coutts *et al.* 2019; Vermeesch 2021). To overcome this limitation, Vermeesch (2021) recommended the use of maximum likelihood ages (MLA), a purely statistical method that employs the maximum likelihood model of Galbraith and Laslett (1993).

In our dataset, MLA provided values of 820 ± 11 Ma for sample SOS-1254, 766 ± 10 Ma for sample SOS-1260 and 786 ± 14 Ma for sample SOS-1274 (see the Supplementary material). These estimates are slightly older than those obtained with the youngest single-grain approach, which returns ages of 808 ± 13, 739 ± 14 and 782 ± 12 Ma, respectively. Nevertheless, they are notably younger than the previously reported MDA of *c.* 900 Ma for the Macururé Complex (Van Schmus *et al.* 2011; Oliveira *et al.* 2015*b*; Neves *et al.* 2019). These new results indicate that the subarkose protoliths of the quartzites were deposited synchronously with, or after, the sedimentation and volcanism of the Novo Gosto unit in the Canindé Domain (Oliveira *et al.* 2015*b*; Passos *et al.* 2022). The minimum depositional age is constrained by the emplacement of the early collisional Camará pluton at 643 ± 2 Ma (Pereira *et al.* 2023).

Sediment dispersal across the Southern Borborema Province

Middle Paleoproterozoic (2000–1980 Ma) and early Neoproterozoic (1000–900 Ma) ages dominate the detrital zircon record of the analysed quartzites, matching the timing of the Rhyacian Orogeny (2.2–2.0 Ga) and Cariris Velhos event (1.0–0.9 Ga) in the Borborema Province. Scarce Siderian and Neoarchean components stand out from this background. We compiled and compared published U–Pb zircon and Sm–Nd whole-rock data from surrounding geological domains to interpret these results and identify potential sediment sources.

The northernmost segment of the São Francisco Craton records several zircon-forming events from the Mesoarchean to the Rhyacian. Protolith crystallization of migmatites and granulites occurred during 2.83–2.73, 2.58–2.47 and 2.18–2.15 Ga, followed by migmatization coeval with granulite-facies metamorphism at 2.08–2.07 Ga (Oliveira 2012, 2014; Santiago *et al.* 2018; Rosa *et al.* 2020). The last magmatic episode in the area corresponds to the emplacement of the acidic–intermediate Arauá dyke swarm at 2.0 Ga (Barbosa *et al.* 2018).

Despite the abundance of Rhyacian ages in the studied quartzites, Archean grains are virtually absent in the Macururé Complex (Van Schmus *et al.* 2011; Oliveira *et al.* 2015*b*; Neves *et al.* 2019), indicating negligible or no cratonic contribution (Fig. 8a). This interpretation is consistent with the Nd isotopic evidence. Sm–Nd data obtained by Oliveira *et al.* (2015*b*) for the metasedimentary units of the Macururé Complex yielded Nd-T_{DM} model ages ranging from 1.8 to 1.3 Ga, which are notably different from those observed in the São Francisco Craton (Fig. 8b, c). The predominance of Tonian and Paleoproterozoic ages, combined with young Nd-T_{DM} model ages, points to derivation from the Borborema Province, possibly linked to the erosion of nearby sources such as the Poço Redondo, Marancó and PEAL domains.

The basement of the Borborema Province is mainly composed of Paleoproterozoic orthogneisses and migmatites related to accretionary and collisional processes that took place during the Rhyacian Orogeny (Caxito *et al.* 2020*a*; Neves 2021). The most likely candidate as a source area for the Paleoproterozoic age fraction identified in the Macururé quartzites is the Jirau do Ponciano Dome (Fig. 8a). It comprises amphibolites (tholeiite to calc-alkaline basalt–andesite) and acidic metavolcanic (calc-alkaline dacite–rhyolite) rocks showing U–Pb zircon ages between 2.07 and 2.05 Ga, interleaved with paragneisses that carry Mesoarchean and Siderian grains (Lima *et al.* 2019). Alternatively, the UHT diatexites from the Arapiraca Complex (2.03–1.96 Ga: Tesser *et al.* 2022) also constitute a plausible source of zircon grains, principally for the younger ones.

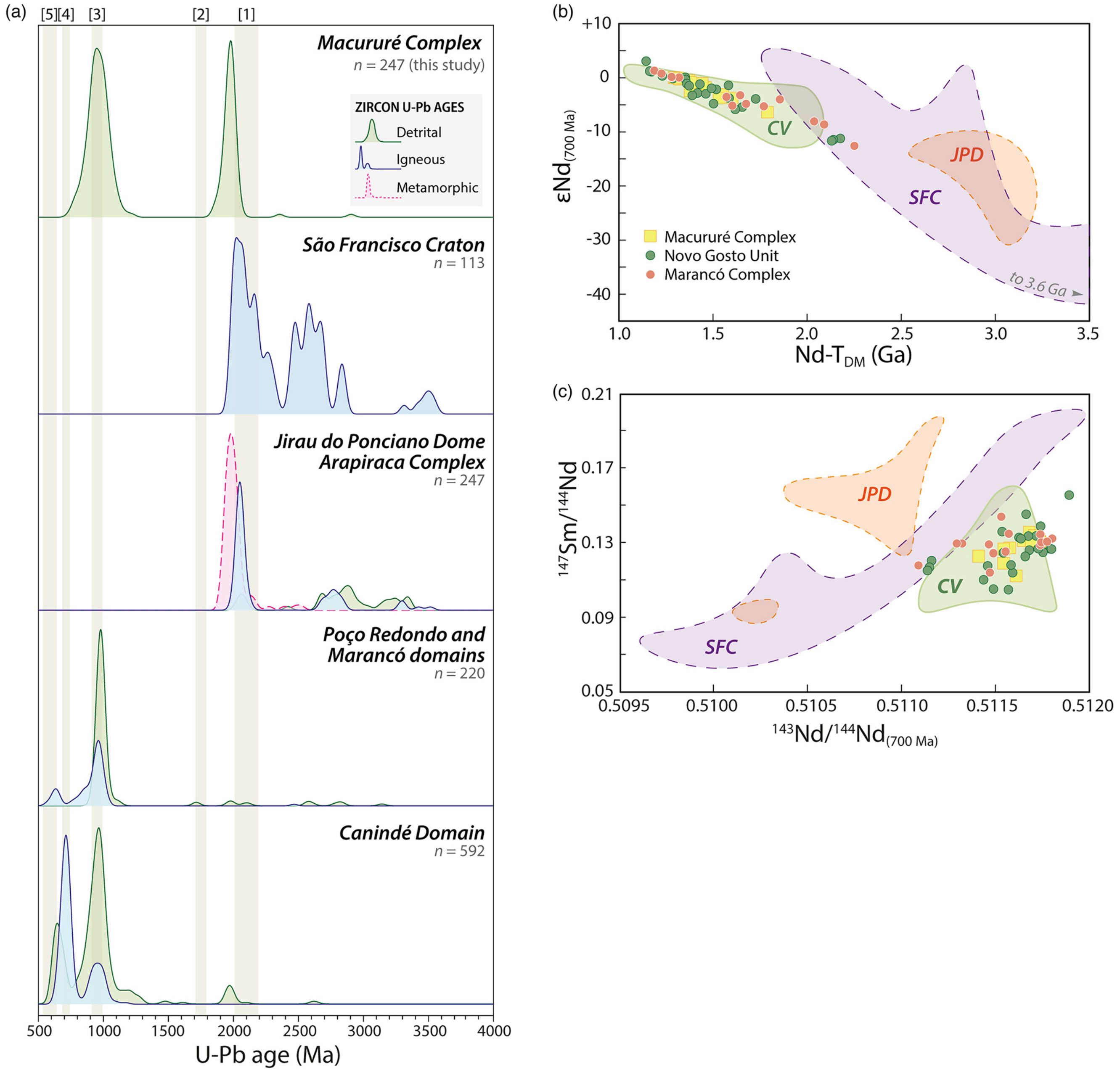

Fig. 8. Potential source areas for metasedimentary rocks of the Macururé Complex. (**a**) Kernel density estimation (KDE) plots for the main pre-Brasiliano crustal compartments in the Borborema Province, envisaged as potential sources for the studied quartzites. Compiled U–Pb data for detrital, igneous and metamorphic grains were filtered by discordance (≤±10%) and best age (^{206}Pb/^{238}U age < 1500 Ma and ^{206}Pb/^{207}Pb age > 1500 Ma) in agreement with our dataset. Vertical bars indicate the main zircon-forming events recorded in the Borborema Province: [1] Rhyacian Orogeny (2.2–2.0 Ga); [2] Statherian taphrogeny (1.8–1.7 Ga); [3] Cariris Velhos event (1.0–0.9 Ga); [4] Canindé event (740–680 Ma); and [5] Brasiliano Orogeny (650–530 Ma). Plots of (**b**) Nd-T_{DM} model ages v. $\varepsilon_{Nd(700\ Ma)}$ and (**c**) ^{143}Nd/^{144}Nd$_{(700\ Ma)}$ v. ^{147}Sm/^{144}Nd comparing the isotopic signature of metasedimentary rocks from the Macururé, Marancó and Canindé domains with potential source areas. Source: (a) São Francisco Craton (Oliveira 2014; Barbosa *et al*. 2018; Santiago *et al*. 2018; Rosa *et al*. 2020), Arapiraca Complex (Tesser *et al*. 2022), Jirau do Ponciano Dome (Lima *et al*. 2019), Poço Redondo and Marancó domains (Carvalho 2005; Oliveira *et al*. 2015*a*, *b*), and Canindé Domain (Lima *et al*. 2018; Pinto *et al*. 2020; Passos *et al*. 2021, 2022); and (b) and (c) São Francisco Craton (Van Schmus *et al*. 1995; Oliveira 2014; Oliveira *et al*. 2015*b*), Jirau do Ponciano Dome (Lima *et al*. 2019), the Cariris Velhos-like source includes data from orthogneisses and metasupracrustal rocks from the Cariris Velhos Belt (Kozuch 2003), and orthogneisses and migmatites from the Poço Redondo and Marancó domains (Oliveira *et al*. 2015*a*, *b*); the isotopic data in (b) and (c) are from Oliveira *et al*. (2015*b*) and Passos *et al*. (2022).

The source of the *c*. 1.1 Ga detritus is intriguing, given the scarcity of magmatic rocks of this age within the Borborema Province. This period correlates with the collisional assembly of the Rodinia supercontinent (Van Schmus *et al*. 2008). A xenocrystic zircon population dated at 1091 ± 13 Ma was described in a 985 Ma metafelsite of granitic composition intercalated with the Riacho Gravatá Complex in the Alto Pajeú Domain (Guimarães *et al*. 2012). Similar detrital ages were documented in the São Caetano Complex (Van Schmus *et al*. 2011; Guimarães *et al*. 2012). These authors suggested that zircon grains older than 1.0 Ga in the region represent an early rifting stage predating the Cariris Velhos event.

Detrital zircon grains in the 1000–900 Ma interval reveal the contribution of Cariris Velhos sources. This event was first recognized in the Central Borborema Province, where metavolcanic rocks and granitic orthogneisses record crystallization ages ranging from *c*. 1000 to 920 Ma (Brito Neves *et al*. 1995; Kozuch 2003).

Other important occurrences of orthogneisses and amphibolites have been described in the Riacho do Pontal Belt (1002–956 Ma: Caxito *et al.* 2014; Amaral *et al.* 2023), PEAL (1027–953 Ma: Neves *et al.* 2021*a*; Bezerra *et al.* 2024), and SOS (1006–940 Ma: Carvalho 2005; Passos *et al.* 2022; Lima *et al.* 2024) in Southern Borborema Province. The Poço Redondo migmatite (980–957 Ma) and the Serra Negra orthogneisses (967–940 Ma) are classic representatives of the Cariris Velhos event in the SOS (Fig. 8a). More recently, Passos *et al.* (2022) reported U–Pb ages of 1006–989 Ma for orthoamphibolites and mylonitic gneisses of the Canindé Domain basement. Sm–Nd isotopic signatures of the metasedimentary rocks from the Macururé Complex broadly overlap with the Cariris Velhos source-type field, together with samples from the Marancó Complex and the Novo Gosto unit (Fig. 8b, c). This pattern highlights the significant contribution of Tonian crustal segments to the Neoproterozoic supracrustal sequences of the SOS.

The middle Neoproterozoic ages form a minor population clustering around *c.* 840 Ma, but define a continuum from *c.* 880 to 800 Ma. Although subordinate, this interval is widely recognized in metasedimentary units in the Borborema Province (Guimarães *et al.* 2012; Cruz *et al.* 2014; Silva Filho *et al.* 2014; Neves *et al.* 2015; Basto *et al.* 2019; Passos *et al.* 2022), suggesting that it may correspond to a significant magmatic episode post-dating the Cariris Velhos event. For instance, a metagabbro from the Paulistana Complex of the Riacho do Pontal Belt yielded 883 ± 4 Ma (Caxito *et al.* 2016), while orthogneisses from the Rio Capibaribe Domain (Central Subprovince) and PEAL (Southern Subprovince) provided zircon ages of 869–852 Ma, interpreted as corresponding to the protolith crystallization (Neves *et al.* 2015, 2021*b*). A continental rifting setting has been evoked to explain the intraplate characteristics of these rocks, representing a new attempt to break up the São Francisco palaeoplate (Caxito *et al.* 2016; Neves *et al.* 2021*b*).

The youngest detrital zircon population, with grains as young as 740 Ma, had not previously been reported from the Macururé Complex. The most probable source is the Canindé Domain, whose metagranitic and metamafic rocks are the only units in the Southern Borborema Province recording this time span (Pinto *et al.* 2020; Passos *et al.* 2021, 2022).

In summary, our new geochronological evidence indicates that the Borborema Province to the north was the main source of detritus for the metasedimentary rocks of the Macururé Complex.

Tracing crustal growth and reworking episodes

Our newly acquired Lu–Hf isotopic data were compared with potential crust-forming events across the Borborema Province and neighbouring terranes to investigate the processes of crustal evolution recorded by detrital zircon.

Paleoproterozoic grains record strongly negative to slightly positive $\varepsilon_{Hf}(t)$ values between −15.6 and +0.5, with Hf-T_{DM}^{C} model ages spreading from the Paleoarchean to the Neoarchean between 3.5 and 2.5 Ga (Fig. 6k). The predominance of subchondritic $\varepsilon_{Hf}(t)$ values indicates that reworking ancient crusts was a significant mechanism leading to crustal differentiation during the Rhyacian–Orosirian.

A few grains show chondritic to slightly positive $\varepsilon_{Hf}(t)$ values from 0 to +0.5 and Hf-T_{DM}^{C} mode ages of *c.* 2.5 Ga, pointing to partial melting of a Neoarchean juvenile source. The oldest Hf-T_{DM} (3.5–3.1 Ga) is recorded by seven grains that display strong negative $\varepsilon_{Hf}(t)$ values (−15.6 to −9.0), suggesting crustal reworking of Paleoarchean sources with a contribution, to a lesser extent, of Mesoarchean juvenile material. Remarkably, most Hf-T_{DM} model ages for Paleoproterozoic grains are concentrated around 2.7 Ga, attesting to a significant crustal residence time and a long-term reworking of crustal components.

These inferences agree with the Hf composition recorded by the basement of the Northern Borborema Province (Fig. 9), which points to the reworking of Archean sources for the 2.19–2.07 Ga granitoids from the Troia Massif (Costa *et al.* 2018). In the Central and Southern sectors of the Borborema Province, the Hf signature of the Paleoproterozoic basement is constrained by inherited zircon populations hosted in Brasiliano granitoids (Lima *et al.* 2021*b*; Brainer *et al.* 2024). The ε_{Hf} values exhibit a wide range, from supra- to subchondritic signatures, which indicate contributions from mixed magma sources, including both mantle-derived and crustal components.

The Hf isotopic signature of the late Mesoproterozoic–middle Neoproterozoic populations is characterized by highly variable subchondritic to suprachondritic $\varepsilon_{Hf}(t)$ values between −24.7 and +8.4, along with Hf-T_{DM} model ages ranging from 3.2 to 1.3 Ga (Fig. 6k). There is no direct relationship between the crystallization age and the Hf composition. Still, the $\varepsilon_{Hf}(t)$ values become progressively more negative towards younger ages, demonstrating the increasing role of reworking processes with time. Positive $\varepsilon_{Hf}(t)$ values are accompanied by the younger Hf-T_{DM}^{C} model ages of *c.* 1.4 and 1.3 Ga, implying a short crustal residence time related to the addition and reworking of newly generated juvenile crust during the Cariris Velhos event.

Likewise, a reworking-based model can account for the Lu–Hf signature observed in Cariris Velhos-related grains. The KDE plot for the Hf-T_{DM}^{C} of this population shows a prominent peak at 1.7 Ga (Fig. 6k). These grains typically retain positive $\varepsilon_{Hf}(t)$ values, aligned with the evolutionary trend depicted by the 1.57 Ga Forquilha protoliths in the Northern Borborema Province (Fig. 9) (Amaral *et al.* 2015). In this context, the mixture of Statherian–Calymmian juvenile crust with older crustal components is a feasible way to explain the observed Hf signature. Pure reworking of Paleoproterozoic–Archean crustal components seems to have been subordinate and is evidenced by older Hf-T_{DM}^{C} and strong negative $\varepsilon_{Hf}(t)$ values.

Regardless of the specific generation model, the crustal evolution processes acting during the Tonian were similar across the Southern Subprovince. This is demonstrated in a plot of crystallization age v. $\varepsilon Hf_{(t)}$ (Fig. 9), where Tonian zircon grains perfectly match the Hf isotopic composition of orthogneisses from the Riacho do Pontal Belt (Caxito *et al.* 2020*b*) and PEAL (Bezerra *et al.* 2024). A good correspondence is also observed with Tonian detrital zircon grains from the Ipueirinha Group (Basto *et al.* 2019) in the Central Subprovince.

Although the data from this study do not include any Ediacaran zircon population, the Lu–Hf compilation indicates that the reworking of pre-existing crust largely dominated the Brasiliano Orogeny (Fig. 9). In contrast, juvenile additions are clearly defined in the northwestern part of the Borborema Province and its African counterpart, the Dahomey Belt (Ganade de Araujo *et al.* 2014; Ganade *et al.* 2016; Pitombeira *et al.* 2021).

The combined U–Pb and Lu–Hf isotopic data for the CAOB align with the crustal trends observed in the Southern Borborema Province (Fig. 9). The parallel vertical arrays are thought to reflect mixing between mantle- and crust-derived components during the Paleoproterozoic, Tonian and Cryogenian–Ediacaran. These similarities suggest that these once-contiguous domains experienced a similar geodynamic evolution.

Lastly, the U–Pb ages and Lu–Hf isotopic signatures in detrital and igneous zircons from the São Francisco Craton significantly differ from those observed in the analysed quartzites (Fig. 9). This region experienced significant additions of new crust during the Paleoarchean, Mesoarchean and Neoarchean (Guadagnin *et al.* 2015; Passos *et al.* 2022; Fachetti *et al.* 2024), partly recorded by the Borborema Province basement (Neves 2021). These findings afford additional support for a non-cratonic derivation of the investigated rocks.

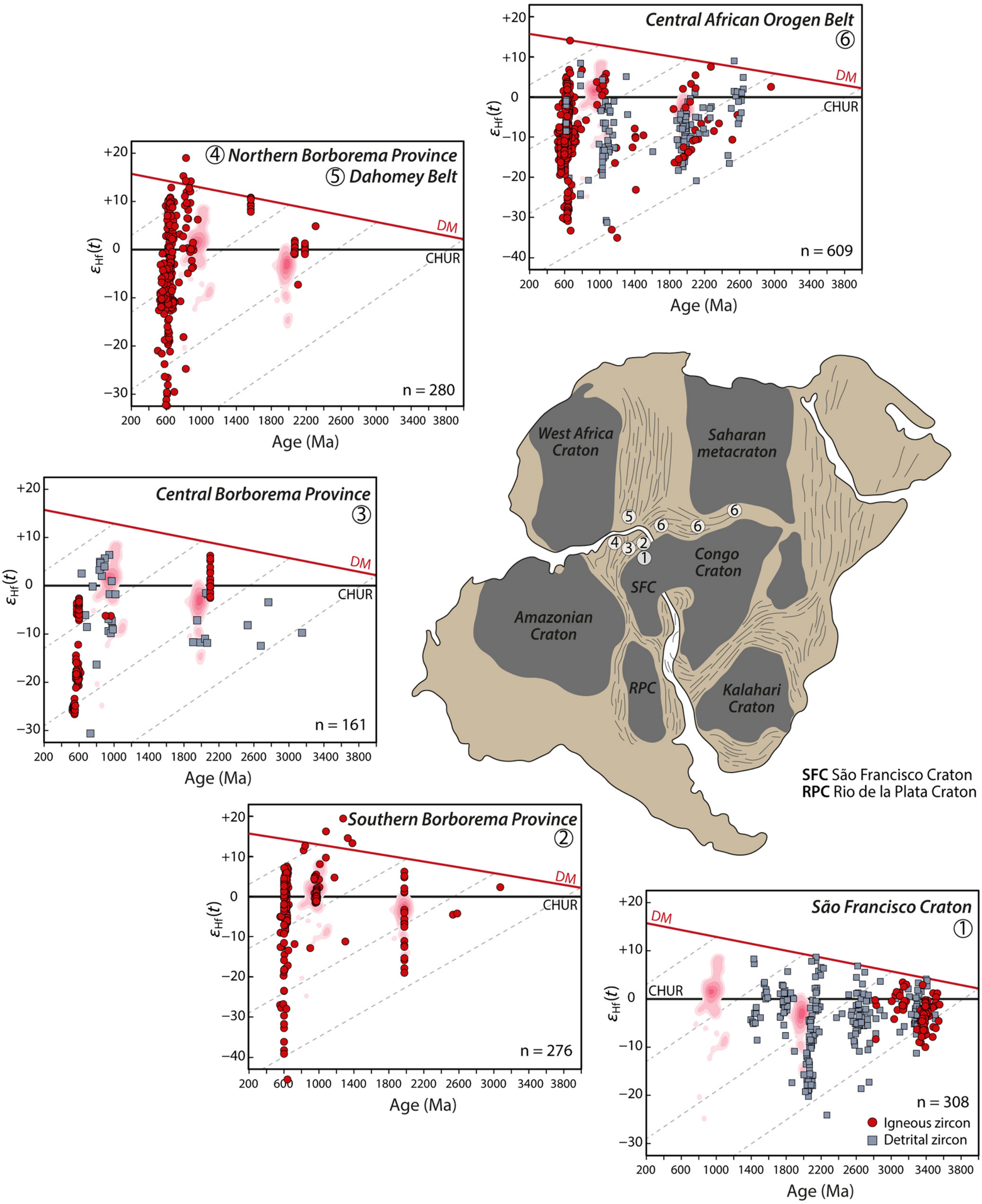

Fig. 9. Crustal evolution of the Southern Boborema Province revealed through Lu–Hf isotopic data compared with neighbouring terranes. The pink areas represent the bivariate kernel density estimation (KDE) of $\varepsilon_{Hf}(t)$ and U–Pb zircon data from the studied samples, including contours of increasing density (25, 50, 75, 90 and 95%). Source: São Francisco Craton (Guadagnin *et al.* 2015; Oliveira *et al.* 2019; Santos *et al.* 2022), Southern Borborema Province (Caxito *et al.* 2020*b*; Pereira *et al.* 2023, 2024; Bezerra *et al.* 2024; Brainer *et al.* 2024), Central Borborema Province (Lima *et al.* 2017, 2021*a*, *b*; Lima 2021; Amorim *et al.* 2018; Basto *et al.* 2019), Northern Boborema Province and Dahomey Belt (Ganade de Araujo *et al.* 2014; Amaral *et al.* 2015; Ganade *et al.* 2016; Costa *et al.* 2018; Pitombeira *et al.* 2021), and Central African Orogenic Belt (Ateh *et al.* 2017; Lima *et al.* 2017; Djerossem *et al.* 2021; Kamguia Kamani *et al.* 2021; Azeuda Ndonfack *et al.* 2022; Ngatcha *et al.* 2022; Yomeun *et al.* 2022).

Tectonic setting for the deposition of metasupracrustal sequences in the SOS

Detrital zircon age distributions are key tools for unravelling the tectonic context of ancient sedimentary basins (Cawood *et al.* 2012), especially when dealing with deformed and metamorphosed sequences, where most stratigraphic relationships are no longer preserved.

Sedimentary basins form in diverse tectonic environments, including convergent, collisional and extensional settings. The difference between the zircon crystallization age (CA) and the depositional age (DA) offers insights into these tectonic settings (Cawood *et al.* 2012). Convergent margin basins typically show more than 30% of zircons with CA – DA < 100 Ma due to the prevalence of arc-derived detritus, resulting in nearly unimodal age spectra. Collisional basins contain 10–50% of zircons with CA – DA < 150 Ma, while extensional settings usually show less than 5%, reflecting limited syndepositional magmatism.

We compiled and reprocessed U–Pb detrital zircon data from the SOS metasedimentary sequences using the filters for best age, discordance and MDA applied in this work, intending to evaluate their tectonic significance in the evolution of the Southern Borborema Province.

Marancó Domain

The KDE plot for all metasedimentary units from the Marancó Domain displays a unimodal distribution of detrital ages with a peak at 960 Ma, close to the MDA of 954–915 Ma (Fig. 10a). Older components are subordinate. This behaviour resembles the age distribution patterns observed in sedimentary deposits emplaced along active continental margins (Fig. 10b) (Cawood *et al.* 2012).

An orogenic context was initially proposed for the Cariris Velhos event in the Southern (Carvalho 2005; Oliveira *et al.* 2010; Caxito *et al.* 2014) and Central (Kozuch 2003; Van Schmus *et al.* 2011) Borborema Province. Nevertheless, the dominance of bimodal magmatism, granitoids with A-type affinities and the absence of Tonian metamorphism argue in favour of an extensional origin for the magmatism in an intraplate environment (Guimarães *et al.* 2012, 2016; Neves *et al.* 2021*a*; Lima *et al.* 2024). Lima *et al.* (2024) proposed that the 940 Ma Serra Negra A-type granites from the Marancó Domain were generated by the partial melting of calc-alkaline granitoids triggered by underplated basaltic magmas in an extensional setting. They further suggest that rift-related normal faulting may have uplifted and exhumed Tonian rocks in the area, making them susceptible to erosion and thus supplying detritus to the metasedimentary rocks of the Marancó Complex. A rift basin model effectively explains the detrital zircon signal of the Marancó Complex, consistent with environments where basin-margin sediments are sourced predominantly from erosion of the adjacent rift shoulder (Olierook *et al.* 2019). In this model, alluvial fans play an important role in promoting the erosion of rift flanks and the incision and recycling of older alluvial fans, rendering a strong margin provenance signal.

Canindé Domain

Detrital age spectra of the Novo Gosto unit are dominated by Tonian zircons (*c.* 950 Ma), with subordinate Ediacaran (*c.* 640 Ma) and Rhyacian (*c.* 2000 Ma) peaks (Fig. 10c). The Canindé Domain comprises amphibolites derived from tholeiitic basalts (Novo Gosto, 743 Ma; Gentileza, 701 Ma), interleaved with clastic sediments yielding an MDA of 625 Ma. Mafic volcanism coincided with the emplacement of gabbroic intrusions (719–704 Ma) and A-type rapakivi granites (720–708 Ma) (Nascimento 2005; Pinto *et al.* 2020; Passos *et al.* 2022).

Passos *et al.* (2022) proposed an accretionary setting (740–680 Ma) for this region, marked by arc-related magmatism and back-arc volcanism–sedimentation represented by the Novo Gosto unit. However, the lack of near-depositional zircon ages weakens this interpretation (Fig. 10c). In addition, Oliveira *et al.* (2015*b*) identified *c.* 39% Cryogenian–Ediacaran zircon grains in a metagreywacke from the Novo Gosto unit, supporting sedimentation coeval with Brasiliano magmatism.

These observations align better with an extensional setting, as previously proposed by Nascimento (2005) and Oliveira *et al.* (2010). The bimodal association of basaltic and rhyolitic magmas, lacking intermediate terms, is typical of rift environments (Frost and Frost 2019). The Canindé gabbros show trace element signatures akin to continental flood basalts (Tarney and Jones 1994), while associated granitoids display A-type, within-plate geochemical affinities (Nascimento 2005). Pillow-like amphibolites suggest that the basin may have evolved into a proto-ocean (Oliveira *et al.* 2010). The short interval between deposition and metamorphism, linked to a tectonic switch from extension to compression, supports the model of rift inversion. In this context, the near-depositional detrital zircon population can be interpreted as derived from synrift magmatism.

Macururé Domain

The sedimentary record of the Macururé Domain has been interpreted as deep-marine deposits of a passive margin on the São Francisco–Congo palaeoplate (D'el-Rey Silva 1999), as a basin adjacent to the presumed Poço Redondo–Marancó arc (Carvalho 2005), and as a passive margin of the PEAL (Oliveira *et al.* 2010).

Our detrital zircon data, combined with previous studies (Van Schmus *et al.* 2011; Oliveira *et al.* 2015*b*; Neves *et al.* 2019) reveal a heterogeneous signature with strong Paleoproterozoic and Tonian signals (Fig. 10e). CA – DA values are <150 Ma for 5% and >100 Ma for 30% of the youngest grains, consistent with a collisional setting (Fig. 10f). However, this interpretation conflicts with the regional tectonic context, as the collisional zone developed in the SOS between 630 and 625 Ma. In addition, the dominance of older detritus aligns more closely with deposition in an extensional setting.

A distinctive zircon population dated to *c.* 780–740 Ma, identified for the first time in the studied quartzites, is contemporaneous with volcanism in the adjacent Canindé Domain, suggesting a possible spatial and temporal connection. Given the synorogenic nature of sedimentation in the Canindé Domain, exhumation and erosion of its rocks are unlikely sources for this detritus. A more plausible explanation involves a shared palaeodrainage system that enabled sediment transport between the two domains. This is supported by similar Sm–Nd signatures between the Macururé Complex and the Novo Gosto unit (Fig. 8b, c) and by the subrounded shapes of the younger grains, which suggest a short-distance transport from proximal sources.

Vaza Barris and Estância domains

KDE and CA – DA plots for the Vaza Barris (Fig. 10g, h) and Estância (Fig. 10i, j) domains reveal marked shifts in provenance from the base to the top of the successions.

The Juetê Formation (JP-159F) in the Estância Domain and the Itabaiana Formation (FS-113) in the Vaza Barris Domain show dominant Paleoproterozoic peaks with minor Archean contributions, and MDA values of 2072 and 1965 Ma, respectively. These samples plot in the collisional and convergent fields, suggesting a direct relationship with the structuring of the Rhyacian Orogen in the São Francisco Craton.

On the other hand, an extensional setting is inferred for the Ribeirópolis (FS-104) and Palestina (FS-166) formations

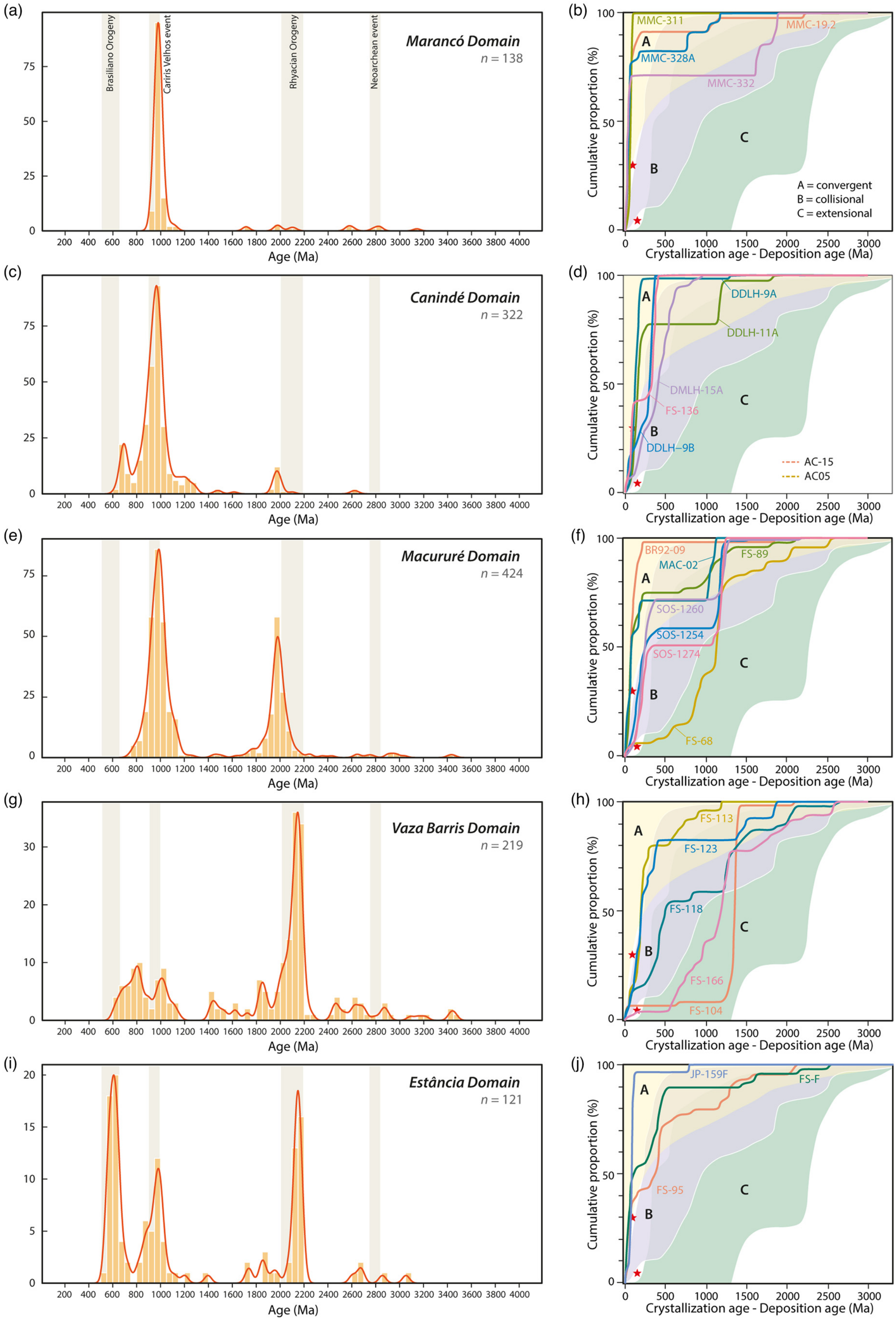

Fig. 10. Kernel density estimation (KDE) plots and cumulative proportion curves showing the difference between the measured crystallization age for detrital zircon grains and the depositional age of the succession in which they occur (Cawood *et al.* 2012) for the metasedimentary samples of the (**a**) and (**b**) Marancó, (**c**) and (**d**) Canindé, (**e**) and (**f**) Macururé, (**g**) and (**h**) Vaza Barris, and (**i**) and (**j**) Estância domains. The youngest single grain of each sample (see Supplementary Table S1) was taken as the maximum depositional age.

(Fig. 10h), deposited after *c.* 875 and 798 Ma, respectively. Carbonates resting above the diamictites of the Ribeirópolis, Juetê and Palestina formations record $^{87}Sr/^{86}Sr$ ratios consistent with late Neoproterozoic seawater and $\delta^{13}C$ values typical of post-glacial carbonates (Sial *et al*. 2010).

The uppermost units (Frei Paulo FS-118, Lagarto FS-F and Palmares JP-159F) display a high proportion of zircon grains approximating the depositional age and plot within the collisional field (Fig. 10h–j). Youngest zircon ages between 615 and 550 Ma imply sedimentation post-dating the collisional phase in the SOS, suggesting derivation from the orogen itself. Therefore, these units are likely to represent deposits of a peripheral foreland basin, as proposed by Oliveira *et al*. (2015*b*).

Pre-orogenic connection and Western Gondwana assembly

The São Francisco Craton and the Borborema Province basement formed part of a Rhyacian orogenic continent, later affected by intermittent rifting (Ganade *et al*. 2021; Neves 2021). The detrital record in the SOS metasedimentary sequences reflects successive stages of this evolution.

Until the early Neoproterozoic, the São Francisco Craton remained a coherent landmass. Between 940 and 910 Ma, plume-related mafic dykes intruded the craton (Evans *et al*. 2016; Chaves *et al*. 2019), coinciding with A-type granite emplacement in the SOS (Lima *et al*. 2024). The erosion of Tonian rocks supplied detritus to the Marancó Complex, yielding unimodal detrital signals and Sm–Nd isotopic signatures resembling those of Cariris Velhos sources.

After a magmatic lull, bimodal magmatism (*c.* 740–680 Ma) and clastic sedimentation took place in the Canindé Domain above a stretched Tonian crust (Nascimento 2005; Passos *et al*. 2022). In this probable rift environment (Oliveira *et al*. 2010), Tonian proximal sources are likely to have acted as topographical highs, becoming the primary source for the sedimentary rocks in the Macururé and Canindé domains.

In the Estância and Vaza Barris domains, sedimentation occurred along the northern margin of the São Francisco palaeoplate. Craton-derived detritus dominated the sedimentation of the basal units, followed by Cryogenian carbonates that record the marine incursions within the rift.

Magmatic activity resumed at *c.* 640 Ma, during the beginning of the Brasiliano Orogeny, with the emplacement of mafic–intermediate magmas (Pereira *et al*. 2020, 2023, 2024). Geochemical and isotopic compositions indicate magma derivation from a lithospheric mantle previously metasomatized by sediments, related to the Rhyacian accretionary events (Pereira *et al*. 2024). Underplating basaltic magmas triggered partial melting of the lower crust, leading to the generation of contemporary I-type granitoids. The ages of the crustal granites (630–625 Ma) of the Macururé Domain currently provide the only constraint on the probable timing of basin inversion and continental collision.

Following the PEAL–SOS collision, orogenic erosion fed the Estância and Vaza Barris foreland basins. The prevalence of detrital zircons younger than 600 Ma in the Lagarto and Palmares formations, with no local magmatic equivalents, points to sediment supply from distal detrital sources via fluvial systems.

Conclusions

The Macururé Complex is a metasedimentary succession dominated by phyllites, metarhythmites, metagreywackes, schists and quartzites. Geochemical data indicate that the quartzites represent compositionally mature, recycled sedimentary deposits, whereas phyllites, metarhythmites, metagreywackes and schists are derived from immature, first-cycle sediments. U–Pb dating of detrital zircons has revealed a bimodal age distribution with prominent Tonian (1000–950 Ma) and Rhyacian–Orosirian (2000–1980 Ma) components, correlating with major tectonic events in the Borborema Province, notably the Cariris Velhos event and the Rhyacian Orogeny. Lu–Hf isotopic data show that the Paleoproterozoic zircons reflect the reworking of Archean crust ($\varepsilon_{Hf}(t)$ −15.6 to +0.5 and Hf-T^{C}_{DM} 3.5–2.5 Ga), while the younger Tonian zircons ($\varepsilon_{Hf}(t)$ −24.7 to +8.4 and Hf-T^{C}_{DM} 3.2–1.3 Ga) indicate both juvenile crust addition and crustal reworking during the Cariris Velhos event. The youngest detrital zircons (*c.* 808–739 Ma) suggest sediment deposition concurrent with magmatism in the adjacent Canindé Domain. Sm–Nd isotopic similarities between the Macururé and Canindé domains further support a shared provenance linked to the wholesale erosion of Cariris Velhos terranes. An extensional tectonic setting is proposed for the sedimentation of these units, with spatially and temporally coeval deposition.

Scientific editing by Roberta Mary Vidotti

Acknowledgements FSP thanks Luísa Dias Barros (PPGG/UFPA) and Jenny Alexandra Ortega Cardozo (SGB/Belém) for their support in obtaining CL images using SEM. The authors are grateful for the valuable comments and suggestions provided by Dr Francisco Hilario Bezerra, Dr Alanielson Ferreira and the anonymous reviewer, which have significantly improved the quality of this manuscript. They also thank the Guest Editor, Dr Roberta Vidotti, for her careful handling of the review process and constructive feedback.

Author contributions **FSP**: conceptualization (lead), visualization (lead), writing – original draft (lead), writing – review & editing (lead); **J-ML**: funding acquisition (equal), resources (lead), validation (lead), writing – review & editing (supporting); **MLSR**: project administration (equal), supervision (equal), validation (equal), writing – review & editing (supporting); **HC**: formal analysis (equal), funding acquisition (equal), validation (equal), writing – review & editing (supporting); **JMMN**: formal analysis (supporting), methodology (lead), software (lead), writing – review & editing (supporting); **MMM**: data curation (supporting), formal analysis (supporting).

Funding This work was funded by the Coordenação de Aperfeiçoamento de Pessoal de Nível Superior (grant no. 001 awarded to FSP) and by the Conselho Nacional de Desenvolvimento Científico e Tecnológico (grant no. 310740/2021-5 awarded to HC, nos 312393/2020-2 and 42625/2018-7 awarded to J-ML and no. 311023/2021-5 awarded to MLSR).

Competing interests The authors declare that they have no known competing financial interests or personal relationships that could have appeared to influence the work reported in this paper.

Data availability All data generated or analysed during this study are included in this published article (and if present, its supplementary information files).

References

Amaral, W., Santos, T.J., Ancelmi, M.F., Fuck, R.A., Dantas, E.L., Matteini, M. and Moreto, C.P. 2015. 1.57 Ga protolith age of the Neoproterozoic Forquilha eclogites, Borborema Province, NE-Brazil, constrained by U–Pb, Hf and Nd isotopes. *Journal of South American Earth Sciences*, **58**, 210–222, https://doi.org/10.1016/J.JSAMES.2014.10.001

Amaral, W.S., Santos, F.H., Martins de Sousa, D.F., Perpétuo, M.P., Brito Neves, B.B., Pitombeira, J.P.A. and Martins, D.T. 2023. A complex history of extension, subduction and collision in west Gondwana: Clues from the Riacho do Pontal orogen, Borborema Province (NE Brazil). *Journal of South American Earth Sciences*, **125**, https://doi.org/10.1016/j.jsames.2023.104297

Amorim, J.V.A., Guimarães, I.P., Farias, D.J.S., Lima, J.V., Santos, L., Biondo, V. and Brainer, C. 2018. Late-Neoproterozoic ferroan granitoids of the Transversal subprovince, Borborema Province, NE Brazil: petrogenesis and geodynamic implications. *International Geology Review*, **61**, 1745–1767, https://doi.org/10.1080/00206814.2018.1544936

Andersen, T., Kristoffersen, M. and Elburg, M.A. 2018. Visualizing, interpreting and comparing detrital zircon age and Hf isotope data in basin analysis – a

graphical approach. *Basin Research*, **30**, 132–147, https://doi.org/10.1111/BRE.12245
Ateh, K.I., Suh, E.S., Shemang, E.M., Vishiti, A., Tata, E. and Chombong, N.N. 2017. New LA-ICP-MS U–Pb ages, Lu–Hf systematics and REE characterization of zircons from a granitic pluton in the Betare Oya Gold District, SE Cameroon. *Journal of Geosciences and Geomatics*, **5**, 267–2683, https://pubs.sciepub.com/jgg/5/6/2
Azeuda Ndonfack, K.I., Xie, Y., Zhong, R., Yomeun, B.S., Cui, K. and Shan, X. 2022. Tectonic evolution of Neoproterozoic rocks, eastern Cameroon: Implication for gold mineralization in the Bétaré Oya and Woumbou–Colomine–Kette districts. *Precambrian Research*, **368**, https://doi.org/10.1016/j.precamres.2021.106475
Bahlburg, H. and Dobrzinski, N. 2011. A review of the Chemical Index of Alteration (CIA) and its application to the study of Neoproterozoic glacial deposits and climate transitions. *Geological Society, London, Memoirs*, **36**, 81–92, https://doi.org/10.1144/M36.6
Barbosa, J.S.F., Marinho, M.M. *et al.* 2018. As raízes granulíticas do cinturão Salvador-Esplanada-Boquim, Cráton do São Francisco, Bahia-Sergipe, Brasil. *Geologia USP. Série Científica*, **18**, 103–128, https://doi.org/10.11606/issn.2316-9095.v18-134238
Basto, C.F., Caxito, F.A. *et al.* 2019. An Ediacaran back-arc basin preserved in the Transversal Zone of the Borborema Province: Evidence from geochemistry, geochronology and isotope systematics of the Ipueirinha Group, NE Brazil. *Precambrian Research*, **320**, 213–231, https://doi.org/10.1016/j.precamres.2018.11.002
Bezerra, J.P.S., Neves, S.P., França, R.H.M., Bruguier, O., Bosch, D. and Moreira, H. 2024. Tonian rifting coeval with the last stages of amalgamation of Rodinia: Evidence from southern Borborema province, northeastern Brazil. *Journal of South American Earth Sciences*, **134**, https://doi.org/10.1016/j.jsames.2023.104741
Brainer, C.C.G., Guimarães, I.P., Silva Filho, A.F., Lima, J.V., Lana, C., Amorim, J.V.A. and Silva, A.A.P. 2024. Peraluminous leucogranites generation during different stages of the Brasiliano Orogeny in the Borborema Province, NE Brazil. *Journal of South American Earth Sciences*, **133**, https://doi.org/10.1016/j.jsames.2023.104663
Brito Neves, B.B., Van Schmus, W.R., Santos, E.J., Campos Neto, M.C. and Kozuch, M. 1995. O evento Carirís Velhos na Província Borborema: intergração de dados, implicações e perspectivas. *Revista Brasileira de Geociências*, **25**, 279–296, https://doi.org/10.25249/0375-7536.1995279296
Brito Neves, B.B., Santos, E.J. and Van Schmus, W.R. 2000. Tectonic history of the Borborema Province, Northeastern Brazil. *In*: Cordani, U.G., Milani, E.J., Thomaz Filho, A. and Campos, D.A. (eds) *Tectonic Evolution of South America*. Sociedad Brasileira de Geologia (SBG), São Paulo, Brazil, 151–182.
Bucher, K. and Grapes, R. 2011. *Petrogenesis of Metamorphic Rocks*. 8th edn. Springer, Berlin, https://doi.org/10.1007/978-3-540-74169-5
Bueno, J.F., Souza, J.J., Araújo, M.N.C. and Oliveira, E.P. 2009. Evolução tectono-cronológica da estrutura de interferência de Nossa Senhora de Lourdes, Faixa Sergipana, NE-Brasil. *Revista Brasileira de Geociências*, **39**, 608–623, https://doi.org/10.25249/0375-7536.2009394608623
Carvalho, M.J. 2005. *Evolução Tectônica Do Domíno Marancó-Poço Rendondo: Registro Das Orogêneses Cariris Velhos e Brasiliana Na Faixa Sergipana, NE Do Brasil*. PhD thesis, Universidade de Campinas, Campinas, São Paulo, Brazil.
Castaing, C., Feybesse, J.L., Thiéblemont, D., Triboulet, C. and Chèvremont, P. 1994. Palaeogeographical reconstructions of the Pan-African/Brasiliano orogen: closure of an oceanic domain or intracontinental convergence between major blocks? *Precambrian Research*, **69**, 327–344, https://doi.org/10.1016/0301-9268(94)90095-7
Cawood, P.A., Hawkesworth, C.J. and Dhuime, B. 2012. Detrital zircon record and tectonic setting. *Geology*, **40**, 875–878, https://doi.org/10.1130/G32945.1
Caxito, F.A., Uhlein, A. and Dantas, E.L. 2014. The Afeição augen-gneiss Suite and the record of the Cariris Velhos Orogeny (1000–960 Ma) within the Riacho do Pontal fold belt, NE Brazil. *Journal of South American Earth Sciences*, **51**, 12–27, https://doi.org/10.1016/j.jsames.2013.12.012
Caxito, F.A., Uhlein, A., Dantas, E.L., Stevenson, R., Salgado, S.S., Dussin, I.A. and Sial, A.N. 2016. A complete Wilson Cycle recorded within the Riacho do Pontal Orogen, NE Brazil: Implications for the Neoproterozoic evolution of the Borborema Province at the heart of West Gondwana. *Precambrian Research*, **282**, 97–120, https://doi.org/10.1016/j.precamres.2016.07.001
Caxito, F.A., Santos, L.C.M.L., Ganade, C.E., Bendaoud, A., Fettous, E. and Bouyo, M.H. 2020*a*. Toward an integrated model of geological evolution for NE Brazil-NW Africa: the Borborema Province and its connections to the Trans-Saharan (Benino-Nigerian and Tuareg shields) and Central African orogens. *Brazilian Journal of Geology*, **50**, e20190122, https://doi.org/10.1590/2317-4889202020190122
Caxito, F.A., Santos, L.C.M.L., Uhlein, A., Dantas, E.L., Alkmim, A.R. and Lana, C. 2020*b*. New U–Pb (SHRIMP) and first Hf isotope constraints on the Tonian (1000–920 Ma) Cariris Velhos event, Borborema Province, NE Brazil. *Brazilian Journal of Geology*, **50**, e20190082, https://doi.org/10.1590/2317-4889202020190082
Chaves, A.O., Ernst, R.E., Söderlund, U., Wang, X. and Naeraa, T. 2019. The 920–900 Ma Bahia-Gangila LIP of the São Francisco and Congo cratons and link with Dashigou-Chulan LIP of North China craton: New insights from U–Pb geochronology and geochemistry. *Precambrian Research*, **329**, 124–137, https://doi.org/10.1016/j.precamres.2018.08.023
Condie, K.C. 1993. Chemical composition and evolution of the upper continental crust: Contrasting results from surface samples and shales. *Chemical Geology*, **104**, 1–37, https://doi.org/10.1016/0009-2541(93)90140-E
Corfu, F. 2003. Atlas of zircon textures. *Reviews in Mineralogy and Geochemistry*, **53**, 469–500, https://doi.org/10.2113/0530469
Costa, F.G., Klein, E.L. *et al.* 2018. Geochemistry and U–Pb–Hf zircon data for plutonic rocks of the Troia Massif, Borborema Province, NE Brazil: Evidence for reworking of Archean and juvenile Paleoproterozoic crust during Rhyacian accretionary and collisional tectonics. *Precambrian Research*, **311**, 167–194, https://doi.org/10.1016/j.precamres.2018.04.008
Coutts, D.S., Matthews, W.A. and Hubbard, S.M. 2019. Assessment of widely used methods to derive depositional ages from detrital zircon populations. *Geoscience Frontiers*, **10**, 1421–1435, https://doi.org/10.1016/j.gsf.2018.11.002
Cox, R., Lowe, D.R. and Cullers, R.L. 1995. The influence of sediment recycling and basement composition on evolution of mudrock chemistry in the southwestern United States. *Geochimica et Cosmochimica Acta*, **59**, 2919–2940, https://doi.org/10.1016/0016-7037(95)00185-9
Cruz, R.F.D., Pimentel, M.M., Accioly, A.C.D.A. and Rodrigues, J.B. 2014. Geological and isotopic characteristics of granites from the Western Pernambuco-Alagoas Domain: implications for the crustal evolution of the Neoproterozoic Borborema Province. *Brazilian Journal of Geology*, **44**, 627–652, https://doi.org/10.5327/Z2317488920140004008
Davison, I. and Santos, R.A. 1989. Tectonic evolution of the Sergipano Fold Belt, NE Brazil, during the Brasiliano Orogeny. *Precambrian Research*, **45**, 319–342, https://doi.org/10.1016/0301-9268(89)90068-5
D'el-Rey Silva, L.J.H. 1999. Basin infilling in the southern–central part of the Sergipano Belt (NE Brazil) and implications for the evolution of Pan-African/Brasiliano cratons and Neoproterozoic sedimentary cover. *Journal of South American Earth Sciences*, **12**, 453–470, https://doi.org/10.1016/S0895-9811(99)00034-6
Djerossem, F., Zeh, A., Isseini, M., Vanderhaeghe, O., Berger, J. and Ganne, J. 2021. U–Pb–Hf isotopic systematics of zircons from granites and metasediments of southern Ouaddaï (Chad), implications for crustal evolution and provenance in the Central Africa Orogenic Belt. *Precambrian Research*, **361**, https://doi.org/10.1016/j.precamres.2021.106233
Evans, D.A.D., Trindade, R.I.F. *et al.* 2016. Return to Rodinia? Moderate to high palaeolatitude of the São Francisco/Congo craton at 920 Ma. *Geological Society, London, Special Publications*, **424**, 167–190, https://doi.org/10.1144/SP424.1
Fachetti, F.J.S., Fuck, R.A., Marimon, R.S., Ferreira, A., da Costa, A.C.D. and Hawkesworth, C.J. 2024. Paleoarchean to Neoproterozoic crust formation and migmatization events in the Borborema Province, NE Brazil: Implications for the growth and reworking of the continental crust. *Gondwana Research*, **129**, 75–90, https://doi.org/10.1016/j.gr.2023.12.005
Fedo, C.M., Wayne Nesbitt, H. and Young, G.M. 1995. Unraveling the effects of potassium metasomatism in sedimentary rocks and paleosols, with implications for paleoweathering conditions and provenance. *Geology*, **23**, 921–924, https://doi.org/10.1130/0091-7613(1995)023<0921:UTEOPM>2.3.CO;2
Floyd, P.A. and Leveridge, B.E. 1987. Tectonic environment of the Devonian Gramscatho basin, south Cornwall: framework mode and geochemical evidence from turbiditic sandstones. *Journal of the Geological Society, London*, **144**, 531–542, https://doi.org/10.1144/gsjgs.144.4.0531
Frost, B.R. and Frost, C.D. 2019. *Essentials of Igneous and Metamorphic Petrology*. 2nd edn. Cambridge University Press, Cambridge, UK, https://doi.org/10.1017/9781108685047
Galbraith, R.F. and Laslett, G.M. 1993. Statistical models for mixed fission track ages. *Nuclear Tracks and Radiation Measurements*, **21**, 459–470, https://doi.org/10.1016/1359-0189(93)90185-C
Ganade, C.E., Cordani, U.G., Agbossoumounde, Y., Caby, R., Basei, M.A.S., Weinberg, R.F. and Sato, K. 2016. Tightening-up NE Brazil and NW Africa connections: New U–Pb/Lu–Hf zircon data of a complete plate tectonic cycle in the Dahomey belt of the West Gondwana Orogen in Togo and Benin. *Precambrian Research*, **276**, 24–42, https://doi.org/10.1016/j.precamres.2016.01.032
Ganade, C.E., Lanari, P. *et al.*. 2021. Magmatic flare-up causes crustal thickening at the transition from subduction to continental collision. *Communications Earth & Environment*, **2**, 41, https://doi.org/10.1038/s43247-021-00103-z
Ganade de Araujo, C.E., Cordani, U.G., Weinberg, R.F., Basei, M.A.S., Armstrong, R. and Sato, K. 2014. Tracing Neoproterozoic subduction in the Borborema Province (NE-Brazil): Clues from U–Pb geochronology and Sr–Nd–Hf–O isotopes on granitoids and migmatites. *Lithos*, **202–203**, 167–189, https://doi.org/10.1016/j.lithos.2014.05.015
Gehrels, G. 2011. Detrital zircon U–Pb geochronology: current methods and new opportunities. *In*: Busby, C. and Azor, A. (eds) *Tectonics of Sedimentary Basins: Recent Advances*. Wiley-Blackwell, Chichester, UK, 45–62, https://doi.org/10.1002/9781444347166.ch2
Gehrels, G. 2014. Detrital zircon U–Pb geochronology applied to tectonics. *Annual Review of Earth and Planetary Sciences*, **42**, 127–149, https://doi.org/10.1146/annurev-earth-050212-124012
Griffin, W.L., Belousova, E.A., Shee, S.R., Pearson, N.J. and O'Reilly, S.Y. 2004. Archean crustal evolution in the northern Yilgarn Craton: U–Pb and Hf-

isotope evidence from detrital zircons. *Precambrian Research*, **131**, 231–282, https://doi.org/10.1016/j.precamres.2003.12.011
Guadagnin, F., Chemale Junior, F., Magalhães, A.J.C., Alessandretti, L., Bállico, M.B. and Jelinek, A.R. 2015. Sedimentary petrology and detrital zircon U–Pb and Lu–Hf constraints of Mesoproterozoic intracratonic sequences in the Espinhaço Supergroup: Implications for the Archean and Proterozoic evolution of the São Francisco Craton. *Precambrian Research*, **266**, 227–245, https://doi.org/10.1016/j.precamres.2015.05.027
Guimarães, I.P., Van Schmus, W.R., De Brito Neves, B.B., Bretas Bittar, S.M., Silva Filho, A.F. and Armstrong, R. 2012. U–Pb zircon ages of orthogneisses and supracrustal rocks of the Cariris Velhos belt: Onset of Neoproterozoic rifting in the Borborema Province, NE Brazil. *Precambrian Research*, **192–195**, 52–77, https://doi.org/10.1016/j.precamres.2011.10.008
Guimarães, I.P., Lara de Brito, M.F., Lages, G.A., Silva Filho, A.F., Santos, L. and Brasilino, R.G. 2016. Tonian granitic magmatism of the Borborema Province, NE Brazil: A review. *Journal of South American Earth Sciences*, **68**, 97–112, https://doi.org/10.1016/j.jsames.2015.10.009
Herron, M.M. 1988. Geochemical classification of terrigenous sands and shales from core or log data. *Journal of Sedimentary Research*, **58**, 820–829, https://doi.org/10.1306/212F8E77-2B24-11D7-8648000102C1865D
Hoffman, P.F., Abbot, D.S. *et al.* 2017. Snowball Earth climate dynamics and Cryogenian geology–geobiology. *Science Advances*, **3**, e1600983, https://doi.org/10.1126/sciadv.1600983
Hoskin, P.W.O. and Schaltegger, U. 2003. The composition of zircon and igneous and metamorphic petrogenesis. *Reviews in Mineralogy and Geochemistry*, **53**, 27–62, https://doi.org/10.2113/0530027
Kamguia Kamani, M.S., Wang, W., Tchouankoue, J.P., Huang, S.F., Yomeun, B., Xue, E.K. and Lu, G.M. 2021. Neoproterozoic *syn*-collision magmatism in the Nkondjock region at the northern border of the Congo craton in Cameroon: Geodynamic implications for the Central African orogenic belt. *Precambrian Research*, **353**, https://doi.org/10.1016/j.precamres.2020.106015
Kozuch, M. 2003. *Isotopic and Trace Element Geochemistry of Early Neoproterozoic Gneissic and Metavolcanic Rocks in the Cariris Velhos Orogen of the Borborema Province, Brazil, and Their Bearing on Tectonic Setting*. PhD thesis, University of Kansas, Lawrence, Kansas, USA.
Kroonenberg, S.B. 1990. Geochemistry of quaternary fluvial sands from different tectonic regimes. *Chemical Geology*, **84**, 88–91, https://doi.org/10.1016/0009-2541(90)90172-4
Lages, G.A., Santos, L.C.M.L., Brasilino, R.G., Rodrigues, J.B. and Dantas, E.L. 2019. Statherian–Calymmian (ca. 1.6 Ga) magmatism in the Alto Moxotó Terrane, Borborema Province, northeast Brazil: Implications for within-plate and coeval collisional tectonics in West Gondwana. *Journal of South American Earth Sciences*, **91**, 116–130, https://doi.org/10.1016/j.jsames.2019.02.003
Lima, D.R. 2016. *Caracterização Petrológica e Geoquímica Do Pluton Curituba, Domínio Poço Redondo–Marancó, Cinturão Sergipano*. Master's dissertation, Universidade Federal de Pernambuco, Recife, Pernambuco, Brazil.
Lima, H.M., Pimentel, M.M., Fuck, R.A., Santos, L.C.M.L. and Dantas, E.L. 2018. Geochemical and detrital zircon geochronological investigation of the metavolcanosedimentary Araticum complex, Sergipano Fold Belt: Implications for the evolution of the Borborema Province, NE Brazil. *Journal of South American Earth Sciences*, **86**, 176–192, https://doi.org/10.1016/j.jsames.2018.06.013
Lima, H.M., Pimentel, M.M., Santos, L.C.M.L. and Dantas, E.L. 2019. Isotopic and geochemical characterization of the metavolcano-sedimentary rocks of the Jirau do Ponciano Dome: A structural window to a Paleoproterozoic continental arc root within the Southern Borborema Province, Northeast Brazil. *Journal of South American Earth Sciences*, **90**, 54–69, https://doi.org/10.1016/J.JSAMES.2018.12.002
Lima, J.V., Guimarães, I.deP., Santos, L., Amorim, J.V.A. and Farias, D.J.S. 2017. Geochemical and isotopic characterization of the granitic magmatism along the Remígio–Pocinhos shear zone, Borborema Province, NE Brazil. *Journal of South American Earth Sciences*, **75**, 116–133, https://doi.org/10.1016/j.jsames.2017.02.004
Lima, J.V., Guimarães, I.P., Neves, S.P., Archanjo, C.J., Amorim, J.V.A., Farias, D.J.S. and Martins, J.V. 2021*a*. Multiple sources and multi-stage emplacement of the Esperança Granitic Complex and its relationship with the Patos–Campina Grande shear zone system, Borborema Province – NE Brazil. *Lithos*, **404–405**, https://doi.org/10.1016/j.lithos.2021.106477
Lima, J.V., Guimarães, I.P., Neves, S.P., Basei, M.A.S., Silva Filho, A.F. and Brainer, C.C.G. 2021*b*. Post-collisional, high-Ba–Sr Teixeira Batholith granites: evidence for recycling of Paleoproterozoic crust in the Alto Pajeú domain, Borborema Province – NE-Brazil. *Lithos*, **404–405**, https://doi.org/10.1016/j.lithos.2021.106469
Lima, R.G.L., Pereira, F.S., Rosa, M.L.S. and Conceição, H. 2024. Serra Negra granites as a record of Tonian rifting within the Sergipano Orogenic System, NE Brazil. *Journal of South American Earth Sciences*, **148**, https://doi.org/10.1016/j.jsames.2024.105180
Lima, S.S. 2021. *Integração de dados aerogeofísicos, geocronológicos e de sensoriamento remoto para a caracterização geológica da porção oeste do Batólito Ipojuca-Atalaia (Domínio Pernambuco-Alagoas)*. PhD thesis, Universidade Federal de Pernambuco, Recife, Pernambuco, Brazil.
McDonough, W.F. and Sun, S.S. 1995. The composition of the Earth. *Chemical Geology*, **120**, 223–253, https://doi.org/10.1016/0009-2541(94)00140-4
McLennan, S.M., Hemming, S., McDaniel, D.K. and Hanson, G.N. 1993. Geochemical approaches to sedimentation, provenance, and tectonics. *Geological Society of America Special Papers*, **284**, 21–40, https://doi.org/10.1130/SPE284-p21
Nascimento, R.S. 2005. *Domínio Canindé, Faixa Sergipana, Nordeste Do Brasil: Um Estudo Geoquímico e Isotópico de Uma Sequencia de Rifte Continental Neoproterozóica*. PhD thesis, Universidade Estadual de Campinas, Campinas, São Paulo, Brazil.
Nesbitt, H.W. and Young, G.M. 1982. Early Proterozoic climates and plate motions inferred from major element chemistry of lutites. *Nature*, **299**, 715–717, https://doi.org/10.1038/299715a0
Nesbitt, H.W. and Young, G.M. 1984. Prediction of some weathering trends of plutonic and volcanic rocks based on thermodynamic and kinetic considerations. *Geochimica et Cosmochimica Acta*, **48**, 1523–1534, https://doi.org/10.1016/0016-7037(84)90408-3
Neves, S.P. 2021. Comparative geological evolution of the Borborema Province and São Francisco Craton (eastern Brazil): decratonization and crustal reworking during West Gondwana assembly and implications for paleogeographic reconstructions. *Precambrian Research*, **355**, https://doi.org/10.1016/j.precamres.2021.106119
Neves, S.P., Bruguier, O., Silva, J.M.R., Mariano, G., Silva Filho, A.F. and Teixeira, C.M.L. 2015. From extension to shortening: Dating the onset of the Brasiliano Orogeny in eastern Borborema Province (NE Brazil). *Journal of South American Earth Sciences*, **58**, 238–256, https://doi.org/10.1016/j.jsames.2014.06.004
Neves, S.P., Silva, J.M.R. and Bruguier, O. 2019. The metasedimentary Macururé Complex (Sergipano Belt, Borborema Province, Brazil) in southern Alagoas state: geology and geochronology. *Journal of the Geological Survey of Brazil*, **2**, 17–25, https://doi.org/10.29396/jgsb
Neves, S.P., Bezerra, J.P.S., Bruguier, O. and França, R.H.M. 2021*a*. Evidence for Early Tonian (ca. 1000–940 Ma) continental rifting in southern Borborema Province (NE Brazil): tectonic inheritance and shear zone nucleation during assembly of West Gondwana. *International Geology Review*, **63**, 851–865, https://doi.org/10.1080/00206814.2020.1734877
Neves, S.P., Teixeira, C.M.L. and Bruguier, O. 2021*b*. 870–850 Ma-old magmatic event in eastern Borborema Province, NE Brazil: Another Tonian failed attempt to break up the São Francisco Paleoplate? *Journal of South American Earth Sciences*, **105**, https://doi.org/10.1016/j.jsames.2020.102917
Ngatcha, R.B., Suh, C.E., Okunlola, O.A., Nunoo, S., Ateh, K.I., Elburg, M. and Hofmann, A. 2022. Crustal modelling from Pan-African granites of the Colomine Gold District, SE Cameroon: Insights from zircon U–Pb dating and Lu–Hf isotope systematics. *Journal of African Earth Sciences*, **187**, https://doi.org/10.1016/j.jafrearsci.2021.104441
Olierook, H.K.H., Taylor, R.J.M. *et al.* 2019. Unravelling complex geologic histories using U–Pb and trace element systematics of titanite. *Chemical Geology*, **504**, 105–122, https://doi.org/10.1016/J.CHEMGEO.2018.11.004
Oliveira, E.M. 2014. *Petrografia, Litogeoquímica e Geocronologia Das Rochas Granulíticas Da Parte Norte Do Cinturão Salvador-Esplanada-Boquim, Bahia-Sergipe*. PhD thesis, Universidade Federal da Bahia, Salvador, Bahia, Brazil.
Oliveira, E.P. 2012. Geologia da Faixa Sergipana no Estado da Bahia. *In*: Barbosa, J., Mascarenhas, J.F., Correa Gomes, L.C., Dominguez, J.M.L. and Souza, J.S. (eds) *Geologia Da Bahia: Pesquisa e Atualização*. Companhia Baiana de Pesquisa Mineral (CBPM), Salvador, Bahia, Brazil, 179–190.
Oliveira, E.P., Windley, B.F. and Araújo, M.N.C. 2010. The Neoproterozoic Sergipano Orogenic Belt, NE Brazil: A complete plate tectonic cycle in Western Gondwana. *Precambrian Research*, **181**, 64–84, https://doi.org/10.1016/j.precamres.2010.05.014
Oliveira, E.P., Bueno, J.F., McNaughton, N.J., Silva Filho, A.F., Nascimento, R.S. and Donatti-Filho, J.P. 2015*a*. Age, composition, and source of continental arc- and syn-collision granites of the Neoproterozoic Sergipano Belt, Southern Borborema Province, Brazil. *Journal of South American Earth Sciences*, **58**, 257–280, https://doi.org/10.1016/j.jsames.2014.08.003
Oliveira, E.P., McNaughton, N.J., Windley, B.F., Carvalho, M.J. and Nascimento, R.S. 2015*b*. Detrital zircon U–Pb geochronology and whole-rock Nd-isotope constraints on sediment provenance in the Neoproterozoic Sergipano Orogen, Brazil: From early passive margins to late foreland basins. *Tectonophysics*, **662**, 183–194, https://doi.org/10.1016/j.tecto.2015.02.017
Oliveira, E.P., Talavera, C. *et al.* 2019. Mesoarchaean (2820 Ma) high-pressure mafic granulite at Uauá, São Francisco Craton, Brazil, and its potential significance for the assembly of Archaean supercratons. *Precambrian Research*, **331**, https://doi.org/10.1016/j.precamres.2019.105366
Passos, L.H., Fuck, R.A., Chemale, F., Lenz, C., Pimentel, M.M., Machado, A. and Pinto, V.M. 2021. Neoproterozoic (740–680 Ma) arc–back-arc magmatism in the Sergipano Belt, southern Borborema Province, Brazil. *Journal of South American Earth Sciences*, **109**, https://doi.org/10.1016/j.jsames.2021.103280
Passos, L.H., Fuck, R.A., Junior, F.C., Lenz, C., Porcher, C.C., Pinto, V.M. and Santos, L.C.M.L. 2022. Neoproterozoic pre-collisional events recorded in the Sergipano belt, Southern Borborema Province, West Gondwana. *International Geology Review*, **64**, 1–19, https://doi.org/10.1080/00206814.2022.2054029
Pearce, J.A. 1982. Trace element characteristics of lavas from destructive plate boundaries. *In*: Thorpe, R.S. (ed.) *Andesites: Orogenic Andesites and Related Rocks*. Wiley-Interscience, New York, 525–548.

Pereira, F.S., Rosa, M.L.S., Conceição, H. and Bertotti, A.L. 2020. Age, composition, and source of the Macururé Mafic Suite, Southern Borborema Province, Brazil. *Brazilian Journal of Geology*, **50**, e20190105, https://doi.org/10.1590/2317-4889202020190105

Pereira, F.S., Conceição, H., Rosa, M.L.S., Marinho, M.M., Tassinari, C.C.G., Milhomem Neto, J.M. and Lafon, J.M. 2023. Late Cryogenian–Ediacaran magmatism in southern Borborema Province, NE Brazil: Ages, sources, petrogenesis, and tectonic setting. *Geoscience Frontiers*, **14**, https://doi.org/10.1016/j.gsf.2023.101626

Pereira, F.S., Lafon, J.M. *et al.* 2024. Constraints on the source and petrogenesis of early Ediacaran shoshonitic mafic magmatism and high-K calc-alkaline granitoids in the Sergipano Orogenic System, Borborema Province, Brazil. *Precambrian Research*, **404**, https://doi.org/10.1016/j.precamres.2024.107312

Pinto, V.M., Koester, E. *et al.* 2020. Petrogenesis of the mafic–ultramafic Canindé layered intrusion, Sergipano Belt, Brazil: Constraints on the metallogenesis of the associated Fe–Ti oxide ores. *Ore Geology Reviews*, **122**, https://doi.org/10.1016/j.oregeorev.2020.103535

Pitombeira, J.P.A., Amaral, W.S., Santos, T.J.S., Dantas, E.L. and Fuck, R.A. 2021. A new record of continental arc magmatism in the Ceará Central Domain, Borborema Province (NE Brazil): evidence from the Pacatuba–Maranguape Complex. *Precambrian Research*, **359**, https://doi.org/10.1016/j.precamres.2021.106192

Rollinson, H. and Pease, V. 2021. *Using Geochemical Data: To Understand Geological Processes*. 2nd edn. Cambridge University Press, Cambridge, UK, https://doi.org/10.1017/9781108777834

Rosa, M.L.S., Conceição, J.A., Marinho, M.M., Pereira, F.S. and Conceição, H. 2020. U–Pb SHRIMP dating of the Itabaiana Dome: a Mesoarchean basement inlier (2.83 Ga) in the Sergipano Orogenic System, Borborema Province. *Brazilian Journal of Geology*, **50**, e20190106, https://doi.org/10.1590/2317-4889202020190106

Rubatto, D. 2017. Zircon: the metamorphic mineral. *Reviews in Mineralogy and Geochemistry*, **83**, 261–295, https://doi.org/10.2138/rmg.2017.83.9

Rudnick, R.L. and Gao, S. 2003. Composition of the continental crust. *In*: Holland, H.D. and Turekian, K.K. (eds) *Treatise on Geochemistry, Volume 3*. Elsevier, Amsterdam, 1–64, https://doi.org/10.1016/B0-08-043751-6/03016-4

Santiago, R.C., Leal, A.B., Marinho, M., Argollo, R., Barbosa, J. and Júnior, E.R. 2018. Litogeoquímica e geocronologia dos ortognaisses migmatíticos do Domo de Itabaiana, Sergipe: uma suíte do tipo tonalito, trondhjemito e granodiorito? *Geologia USP. Série Científica*, **17**, 81–98, https://doi.org/10.11606/issn.2316-9095.v17-121838

Santos, C., Zincone, S.A., Queiroga, G.N., Bersan, S.M., Lana, C.C. and Oliveira, E.P. 2022. Evidence for change in crust formation process during the Paleoarchean in the São Francisco Craton (Gavião Block): Coupled zircon Lu–Hf and U–Pb isotopic analyses and tectonic implications. *Precambrian Research*, **368**, https://doi.org/10.1016/j.precamres.2021.106472

Santos, L.R. 2016. *Petrologia Do Stock Canindé Velho, Sistema Orogênico Sergipano, NE Brasil*. Master's dissertation, Universidade Federal de Sergipe, São Cristóvão, Sergipe, Brazil.

Sial, A.N., Gaucher, C. *et al.* 2010. C-, Sr-isotope and Hg chemostratigraphy of Neoproterozoic cap carbonates of the Sergipano Belt, Northeastern Brazil. *Precambrian Research*, **182**, 351–372, https://doi.org/10.1016/j.precamres.2010.05.008

Silva, J.M.R., Campos Neto, M.C. and Brito Neves, B.B. 1995. Deformação e metamorfismo principais de uma parte da Faixa Sul-Alagoana (Complexo Macururé), Sistema de Dobramentos Sergipano, Nordeste do Brasil. *Revista Brasileira de Geociências*, **25**, 343–350, https://doi.org/10.25249/0375-7536.1995343350

Silva Filho, A.F., Guimarães, I.P., Van Schmus, W.R., Armstrong, R.A., Rangel da Silva, J.M., Osako, L.S. and Cocentino, L.M. 2014. SHRIMP U–Pb zircon geochronology and Nd signatures of supracrustal sequences and orthogneisses constrain the Neoproterozoic evolution of the Pernambuco–Alagoas domain, southern part of Borborema Province, NE Brazil. *International Journal of Earth Sciences*, **103**, 2155–2190, https://doi.org/10.1007/s00531-014-1035-4

Soares, H.S., Sousa, C.S., Rosa, M.L.S. and Conceição, H. 2019. Petrologia dos stocks Santa Maria, Monte Pedral, Bom Jardim, Boa Esperança e Niterói, Suíte Intrusiva Serra do Catu, estado de Sergipe, NE Brasil. *Revista Geologia USP. Série Científica*, **19**, 63–84, https://doi.org/10.11606/issn.2316-9095.v19-156598

Tarney, J. and Jones, C.E. 1994. Trace element geochemistry of orogenic igneous rocks and crustal growth models. *Journal of the Geological Society, London*, **151**, 855–868, https://doi.org/10.1144/GSJGS.151.5.0855

Taylor, S.R. and McLennan, S.M. 1985. *The Continental Crust: Its Composition and Evolution. An Examination of the Geochemical Record Preserved in Sedimentary Rocks*. Blackwell Scientific, Oxford, UK.

Tesser, L.R., Ganade, C.E., Weinberg, R.F., Basei, M.A.S., Moraes, R. and Batista, L.A. 2022. Ultrahigh-temperature Palaeoproterozoic rocks in the Neoproterozoic Borborema Province, implications for São Francisco Craton dispersion in NE Brazil. *Journal of Metamorphic Geology*, **40**, 359–387, https://doi.org/10.1111/jmg.12632

Van Schmus, W.R., Brito Neves, B.B., Hackspacher, P. and Babinski, M. 1995. U/Pb and Sm/Nd geochronologic studies of the eastern Borborema Province, Northeastern Brazil: initial conclusions. *Journal of South American Earth Sciences*, **8**, 267–288, https://doi.org/10.1016/0895-9811(95)00013-6

Van Schmus, W.R., Oliveira, E.P., da Silva Filho, A.F., Toteu, S.F., Penaye, J. and Guimaraes, I.P. 2008. Proterozoic links between the Borborema Province, NE Brazil, and the Central African Fold Belt. *Geological Society, London, Special Publications*, **294**, 69–99, https://doi.org/10.1144/SP294.5

Van Schmus, W.R., Kozuch, M. and Brito Neves, B.B. 2011. Precambrian history of the Zona Transversal of the Borborema Province, NE Brazil: Insights from Sm–Nd and U–Pb geochronology. *Journal of South American Earth Sciences*, **31**, 227–252, https://doi.org/10.1016/j.jsames.2011.02.010

Vermeesch, P. 2021. Maximum depositional age estimation revisited. *Geoscience Frontiers*, **12**, 843–850, https://doi.org/10.1016/J.GSF.2020.08.008

Warr, L.N. 2021. IMA–CNMNC approved mineral symbols. *Mineralogical Magazine*, **85**, 291–320, https://doi.org/10.1180/MGM.2021.43

Wilde, S.A., Valley, J.W., Peck, W.H. and Graham, C.M. 2001. Evidence from detrital zircons for the existence of continental crust and oceans on the Earth 4.4 Gyr ago. *Nature*, **409**, 175–178, https://doi.org/10.1038/35051550

Wilson, M. 1989. *Igneous Petrogenesis: A Global Tectonic Approach*. Springer, Dordrecht, The Netherlands, https://doi.org/10.1007/978-1-4020-6788-4

Yomeun, B.S., Wang, W. *et al.* 2022. Geochronology, geochemistry and Sr–Nd, Hf–O isotope systematics of the Linte massif, Adamawa–Yade domain, Cameroon: Implications on the evolution of the Central African Fold Belt. *Precambrian Research*, **375**, https://doi.org/10.1016/j.precamres.2022.106675